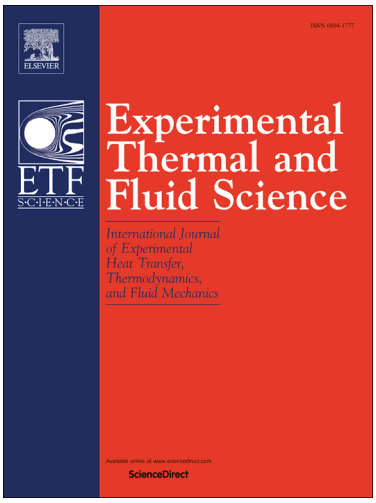


# Determination of thermal contact conductance of flat and curvilinear contacts by transient approach

Surya Kumar, Andallib Tariq

PII: S0894-1777(17)30176-0
DOI: http://dx.doi.org/10.1016/j.expthermflusci.2017.06.004
Reference: ETF 9123

To appear in: *Experimental Thermal and Fluid Science*

Received Date: 7 January 2017
Revised Date: 13 May 2017
Accepted Date: 5 June 2017

Please cite this article as: S. Kumar, A. Tariq, Determination of thermal contact conductance of flat and curvilinear contacts by transient approach, *Experimental Thermal and Fluid Science* (2017), doi: http://dx.doi.org/10.1016/j.expthermflusci.2017.06.004

# Determination of thermal contact conductance of flat and curvilinear contacts by transient approach

**Surya Kumar, Andallib Tariq**[1]
Department of Mechanical and Industrial Engineering,
Indian Institute of Technology Roorkee,
Roorkee, Uttarakhand-247667, INDIA

## ABSTRACT

*Accurate knowledge of the thermal contact conductance (TCC) across fixed metallic contacts of flat-flat as well as curvilinear surfaces is becoming vital for the safety and performance in the critical fields like nuclear energy production, thermal management of electronics packaging, aviation sector, etc. In this regard, a steady state methodology is well acceptable as a reliable approach for estimating the TCC for specimen under pressed contact conditions, which requires long hours of experimental run. Whereas, a transient methodology aims to determine the time varying estimate of TCC or the heat flux related with the specific application areas requires a very short duration experiment. Research works on the estimation of TCC through transient methods are available for only flat-flat contacts. Moreover transient methods have seldom been used for estimating the steady state TCC. Present investigation systematically explore and develop a better understanding of transient methodology towards estimating TCC between flat-flat as well as curvilinear metallic contacts under consistent loading conditions by using the inverse analysis. A sequential function estimation algorithm based on the analytical solution for a semi-infinite body has been used for solving inverse heat conduction problem (IHCP), and subsequently, the transient TCC is determined by using an estimated transient heat flux and an instantaneous temperature jump at the interface. Firstly, the inverse problem has been tested by a numerically generated measurement. Later a customized experimental facility has been used to conduct transient, as well as steady state experiments for flat-flat, cylinder-flat and cylinder-cylinder configurations under similar working parameters. Experimental results of transient heat flux show a quasi-static thermal equilibrium at the end of test run, which form the basis to successfully extract the steady-state TCC measurement with greater reliability. An under prediction in transient TCC up to 60 % is found to be inevitable, if compared against the steady state TCC estimate based upon the linearly extrapolated temperature drop measurements of each contacting specimens. However, a close agreement between the stabilized transient TCC and the steady state TCC has been observed, when steady TCC values are directly based upon the actual interfacial temperature drop measurements without any extrapolation. Eventually, this work establishes the viability of present transient approach in suitably predicting the steady state TCC values of different contact configurations.*

**Keywords**: Thermal contact conductance (TCC), Inverse heat transfer, Transient heat flux, Transient TCC, Steady state TCC, Curvilinear contact.

[1] Corresponding author. Tel.: +91-1332-285728; fax: +91-1332-285665
E-mail address: tariqfme@iitr.ac.in

## 1. Introduction

Accurate knowledge of TCC are becoming important in the major engineering applications ranging from critical areas like nuclear reactor cooling and spacecraft thermal control to the fields of electronics packaging, gas turbine, internal combustion engine cooling, heat exchangers, sample-tool interface, forging and metal forming processes. Due to its immense technological importance, it had been a topic of research from several decades. However, correct evaluation of TCC of any contacting surfaces is a complex phenomenon and can neither be measured nor calculated directly due to the difficulty in estimating the real contact area between the mating surfaces. Variations in real contact area arises due to several parameters i.e. size and distributions of the surface roughness and exact dimensions of the interstitial gap, contacting pressure, microhardness and associated properties of the materials in contact.

Many researchers have carried out their study on thermal contact conductance by using theoretical as well as experimental methods. Some of the pioneer works like CMY model [1] and Mikic model [2] paved the way for analytical works. Predicting TCC, based upon theoretical models is a tough task and still in developing stage due to complexity involved in handling real surface geometries, and associated elastic, plastic and elastoplastic contact mechanics deformation theories; which generally depends upon various simplifying assumptions. In this regard, recent study of Sadowski and Stupkiewicz [3] carries in depth analysis about the limitations of existing theoretical models, which were generally based upon the assumptions, that the fraction of proposed real contact area is relatively small and the contact spots are assumed to be circular and separated. It was argued that these aforesaid two assumptions were not valid in the conditions characterized by large fractions of real contact area, and hence restrict the suitability of existing theoretical models in predicting the TCC for real engineering problems. Therefore, experimental investigations are inevitable [4] in order to get the accurate estimate of TCC at the contact interface for different applications. Conventionally, two types of experimental approaches have been employed to measure TCC which are steady state and transient approaches. Steady sate TCC [4-10] is estimated by calculating the ratio of interfacial heat flux obtained by using Fourier heat conduction to the steady state temperature drop derived on the basis of linear extrapolation of temperature measurement of each contacting specimens, i.e.

$$h = \frac{\dot{q}}{\Delta T} \tag{1}$$

Extensive steady state experimental analysis under various parameters had been performed on flat-flat contacts [4-10] for the estimation of TCC. Veering away from the flat-flat metallic contact, very limited number of experimental steady state TCC investigations were performed on curvilinear contacts, i.e., cylinder-flat and cylinder-cylinder contacts due to their complex

geometrical arrangements [5]. The nature of contact in both of the configuration is line type contact at the interface, rather than the flat surface contact. The value of TCC across cylinder-cylinder and cylinder-flat contacts is an important consideration for the design of a thermal system in an industry. Ayers [11] reported diverse applications of cylindrical contacts such as composite cylindrical tanks, space structures, power transmission lines, electronic devices, nuclear fuel elements, air conditioning systems, and pipelines. Madhusudana [12] presented a steady state analysis for the prediction of the thermal conductance of concentric cylindrical joints for radial heat flow. The value of TCC depends on the geometrical, thermos-physical and surface properties of the cylinders as well as heat flux and maximum operating temperatures. Kumar et al. [13] developed a mathematical model to predict TCC between curvilinear surfaces and conducted steady state experiments in vacuum for the measurement of TCC between stainless steel and aluminum cylindrical contacts over a range of contact pressure. It was found that the value of TCC was of lower magnitude in cylindrical contacts as compared to flat contacts. Mcgee et al. [14] presented a line contact model for the thermal resistance of a cylinder-flat contact, and compared the results with the steady state experimental measurements. It was observed that the validity of line-contact model was dependent on limiting minimal contact loading, and below a certain value of load parameter large errors were reported along the contacting surfaces. Complexity of the field calls for the dismal need towards reliable experimental investigations to estimate the TCC for different curvilinear contacts.

Although, the steady state experimental approach is considered to be a reliable and relatively accurate method [4, 15], but associated with a long waiting time [16]. Contrary to this, the transient approach consist of very short duration test run, and helps in determining the time varying estimate of TCC or the heat fluxes. Transient approach utilizes the transient temperature data in conjunction with the inverse heat conduction problem (IHCP) to estimate the TCC as an unknown boundary condition. The inverse heat conduction method implies that the effect (such as the temperature at interior locations in both the bodies) is utilized to estimate the cause (such as, boundary condition) in terms of heat flux or TCC. IHCP can be described in terms of an optimization problem where the objective function is represented by the squared difference between measured and estimated unknown variables. For the measured variables, the inverse problem normally utilizes the experimental transient temperature measurements at some fixed spatial locations in the contacting bodies to estimate the TCC. Generally, there are two classes of inverse problems, typically known as parameter and function estimation. Beck and Woodbury [17] presented an overview of the general procedure and concepts related to identification of parameters or functions by inverse techniques. Many of the times the estimation of TCC can be made based upon the combined approaches. Comparative studies show that the combined procedure can efficiently and reliably estimate the values of the unknown thermal coefficients, rather than the independent use of each [18, 19].

Several methods are being used to solve IHCP in estimating TCC. One of the most stable algorithms for IHCP in TCC estimation is the iterative technique of optimization by using

conjugate gradient method (CGM) [20-24]. Most of the time, in these investigations the CGM derives basis from the perturbational principles [20] and transforms the inverse problem to the solutions of three problems, namely, the direct problem, the sensitivity problem and the adjoint problem. Whereas, Chen and Tuan [25] applied an on-line inverse solution methodology based on the weighting input estimation to evaluate the interface contact conductance between periodically contacting surfaces from transient temperature measurements. This method demonstrates superior capability in terms of stability, fast convergence and good accuracy over CGM.

Above mentioned transient studies generally use multiple sensors as measured input to IHCPs. It had been observed that the transient temperature response of an internal point in a heat conducting body was lagged as compared to surface of the body due to the damping effect [26]. It was also observed that the lagging was more pronounced for the points located far from the surface. Therefore use of multiple sensors is less effective in damping measurements errors. The major source of uncertainties while using IHCP comes from intrusive way of internal temperature measurements, and use of multiple sensors can largely affect the thermal behavior of heat conducting bodies. Moreover, whole domain estimation procedure which remains at the heart of these IHCPs, are seldom computationally efficient [26]. Because of these characteristics, another class of IHCP based upon the uses of single sensor was also recommended for the IHCP solutions [27]; where the unknown functional form of transient heat flux variation is assumed and the unknown parameters in the assumed functional form are estimated on the basis of sequential function estimation procedure (SFEP) [27].

Evidently, an inverse heat transfer problems are an ill-posed problem and it is very sensitive to measurement errors, therefore the SFEP algorithm uses a regularization method for the stability of its solution. To regularize this algorithm, Beck et al. [27] proposed the use of lesser set of data from the whole set of measurement, where the optimization function, i.e. the heat flux of the un-adopted data set are temporary assumed as constant, and the un-adopted data/measurement are termed as the future time steps/temperatures. The use of several un-adopted measurement as future temperatures data greatly improves the stability of the algorithm and substantially reduces the sensitivity to the measurement errors. The SFEP algorithm has been frequently implemented in accessing the transient interfacial boundary condition in internal combustion engine [16], heat flux in solidification and casting [28], electroslag remelting [29], quenching [30], glass forming process [31], the gap between coolant pump rotor can and rotor [32], etc.; where most of the time the non-linear estimation technique of Beck [33] was adopted as the basis. In most of these application areas, effectiveness of the heat transfer depends upon the heat flow characteristics from the onset of the process, rather than the steady state condition. Therefore, it was of specific interest to found the variation of either the heat flux or heat transfer coefficient with time.

Generally, it was observed that the interfacial heat flux transient rises immediately at the onset of process, and decreases exponentially once it attains the peak. The sharp initial rise in the heat flux were linked with the high heat addition due to the good contact at the onset of various manufacturing processes [28-31], and the peak in the heat flux had been associated with the beginning of respective phase change processes (e.g. nucleate boiling, solidification, etc.) during which the contact becomes non-conforming state which may lead to the formation of a gas gap, resulting in a reduction in heat flux at the interface. Further, the peak heat flux increases with the respective increase in driving force for heat transfer across the interface due to various associated factors, resulting reduced interfacial thermal resistances. Similarly, the experimental investigation of transient heat transfer between specimens with narrow macroscopic gap [32] also showed the same trend even in the variation of TCC with time, i.e. a sharp rise up to a peak value, which decreases gradually with time. In most of these studies, the peak value was taken as the representative point, instead of the whole curve to study the effect of varying parameters.

Evidently, in the application areas related with the various manufacturing processes such as sliding contact, periodic contact, contact with macroscopic gaps, or cyclic loading; the transient behaviour of the occurring heat fluxes, TCR/TCC, and resulting temperature distributions at the interface are of prime importance.

The steady state estimate of TCC is also of critical importance for many other application areas related with nuclear reactors, internal combustion engines, electronic packaging, heat exchangers, bolted joints, cryogenic applications, etc., where there exists the fixed press contact. Evidently, s*teady state TCC* is often estimated by the reliable stationary temperature field measured on the basis of steady state conditions, which is subsequently used to calculate the heat flux through, and the temperature drop along the surface region [4-6]. However, resolving the *steady state TCC* through the *transient methodology* is seldom addressed in literature. In this regard, Fieberg and Kneer [16] tried to estimate the TCC by inverse modelling based on the 1-D analytical solution for a semi-infinite body with the help of very short duration experiments (1.4 sec), while using high speed IR thermography; but the result shows the remarkable deviation from the analytical correlations. Additionally, it consists of ambiguity in picking the representative value of TCC from the TCC variation curve. Later, Burghold et al. [23] have extended the investigation, and performed short duration based transient experiments (1.4 sec) to calculate the instantaneous contact heat transfer by solving the inverse heat conduction problem. A direct relation between the instantaneous load and contact heat transfer coefficient was established while using CGM based finite conduction solution. Comparison between the transient TCC against the TCC during the stabilized steady state load had been shown, and it was found that the oscillation in the TCC values settles all along the peak value of the TCC during this short span, rather than an increasing trend of TCC. Recently Zhu et al. [34] has shown a slow and continuous increasing trend in TCC after the rapid sporadic rise at the onset of contact with the help of relatively longer test time (upto 40 sec). However, concerns were raised that, if

the test time would had been much long enough, can the thermal contact conductance reach a steady state value? The matter might become complex further, especially when it would be performed on the basis of finite conduction modelling while using the multiple sensor based measurements; where using the ratio of the transient heat flux and the interfacial temperature drop variation with time brings further proneness to error towards predicting the TCC.

In most of the aforementioned investigations, a conflicting perspective does occur in selecting the representative value of TCC from its variation curve with respect to the time. Due to different approach towards selecting representative values of TCC during transient methodologies [16, 23, 34], significant deviations in results are inevitable. These underlying issues calls for the need of a comparative study between the transient results against the steady-state contact heat transfer measurements, performed with the same specimen/setup under similar parameter conditions; and thus develop more accurate methodology for predicting *steady state TCC* with transient approach. A survey of the literature shows that the semi-infinite solid approximation has already been examined closely [35] in the context of aerodynamics heat transfer based experiments, where the time variation of the local Nusselt number in the transient experiment for a flat plate has been examined and successfully used towards the estimation of steady state heat transfer coefficients. The potential benefit of the semi-infinite solid approximation in terms of computational efficiency was also recognised against the full differential equation based numerical solution.

In the similar manner, an inverse methodology towards estimating TCC between the metallic contacts under consistent loading conditions has been performed in this work. A single sensor based inverse algorithm has been explored for the estimation of TCC between flat metallic contacts, while using 1-D semi-infinite conduction solution. Algorithm based on sequential function estimation [27] has been used to estimate the unknown boundary condition. Initially, the scheme has been tested successfully with the numerical based temperature results, and subsequently it has been extended towards the estimation of TCC based upon transient temperature measurements. A comprehensive set of experiments on the basis of transient and steady state measurements have been performed on the same specimens with a customized experimental setup [4-6]. The duration of the transient heat transfer experiments were selected judiciously while complying the validity criteria of semi-infinite solid assumption, i.e. the total duration of the transient run should be lesser than the penetration time of the substrate $t \le 0.1x^2/\alpha$ [36]. A simple calculation with the standard thermo-physical properties of specimen under consideration will reveal that the maximum permissible penetration time in the present case is $\le 40$ sec to restrict the farthest temperature change by 1.0%. This condition was further cross-checked against direct thermocouple measurement inside the specimen but located far away from the surface. Subsequently, this paper also establish the suitability of the present inverse approach in predicting transient as well as the steady state TCC between the pressed cylinder-flat and cylinder-cylinder contacts under different axial loading condition. The

comparison of the transient results against the steady state measurements with comprehensive set of investigations on the same and well standardized experimental setup (which has successfully demonstrated its suitability in producing accurate database [4-6] of steady state TCC values) can be treated as the unique strength of present work which is seldom addressed in the literature.

Summarizing the scope of the present work, the paramount objectives of this study are to design and develop a transient experimental procedure (i) to estimate the transient variation of TCC at the onset of heat flow establishment between the pressed thermal contact of different geometrical configurations, (ii) provide valuable insight about the suitable strategy to get an accurate estimate of steady state TCC between the pressed thermal contact while adopting the transient approach, and (iii) provides the benchmark dataset of TCC between some of the unique kind of curvilinear contact configurations of practical relevance, which can also be used towards validating any of the upcoming theoretical models in the pertinent field.

## 2. Numerical implementation

The problem statements and formulation of an IHCP has been described in this section of the article. The objective is to estimate the transient TCC at the interface of two metallic bodies by using an IHCP modelling. A direct problem has been solved for generating simulated temperature data to provide as an input for the solution of IHCP.

### *2.1 Direct problem*

The direct problem involves the determination of temperature distribution in the contacting specimens when the thermos-physical properties, contact conductance, $h$ and the boundary conditions at the outer ends are known. Fig. 1 (a) shows the geometry and the computational grid generation for the one-dimensional heat transfer problem. Geometrical dimensions and physical properties taken to solve the direct problem are summarized in Table 1. The mathematical formulation for this one dimensional heat conduction problem is described by the following general expressions.

$$\frac{\partial^2 T}{\partial x^2} = \frac{1}{\alpha}\frac{\partial T}{\partial t} \qquad (2a)$$

$$\frac{\partial T}{\partial x} = 0,\ at\ x = 0\ \&\ x = L_1 + L_2 \qquad (2b)$$

$$-k\frac{\partial T}{\partial x} = h_{\sup}(t)\left[T_1 - T_2\right],\quad x = L \qquad (2c)$$

$$T = T_i;\quad t = 0 \qquad (2d)$$

Interfacial boundary condition in terms of $h_{sup} = 2.12$ kW/m-K has been provided at the interface in order to make the above formulation well-posed and consequently, Eq. 2 can be solved by finite difference method.

*2.2 Inverse problem*

It is evident that the determination of unknown $h(t)$ is not possible at the inaccessible interface through the solution of direct heat conduction problem. Therefore, the estimation of TCC is based on the solution of IHCP utilizing the temperature data achieved by the solution of direct problem. An SFEP algorithm has been used to solve IHCP problem. It estimates the interfacial heat flux, $\dot{q}(t)$. The estimation of $\dot{q}(t)$ is based on the analytical solution for a semi-infinite body. Schematic of two semi-infinite bodies in contact with single temperature sensor has been depicted in Fig. 1 (b). Although body 1 and body 2 are finite in dimensions, but if the contact span is considered to be extremely short as against the penetration time of the substrate, then the bodies can be treated as being semi-infinite, and the classical solution of semi-infinite conduction problem with prescribed initial surface temperature, and boundary conditions can be used to evaluate the unknown heat flux, $\dot{q}(t)$ at the interface. The governing equation along with boundary and initial conditions for a semi-infinite body, while considering the constant properties can be written as:

$$\begin{aligned} &\frac{\partial T}{\partial t} = \alpha \frac{\partial^2 T}{\partial x^2} \qquad && \frac{\partial T}{\partial x} = 0, \; when \; x \to \infty \\ &\dot{q} = -k \frac{\partial T}{\partial x} \;\; at \; x = 0 \qquad && T(x, t = 0) = T_i \end{aligned} \tag{3}$$

The SFEP algorithm proposed by Beck et al. [27] has been used for the estimation of $\dot{q}(t)$, which is shown below:

$$\dot{q}(t) = \frac{\sum_{i=1}^{r} (Y_{M+i-1} - \hat{T}_{M+i-1}) \Phi_i}{\sum_{i=1}^{r} \Phi_i^2} \tag{4}$$

Eq. (4) optimizes the least square difference between the measured and calculated temperatures at each time step, based on the sensitivity coefficient. With the step response to a unit heat flux jump for a semi-infinite body, the sensitivity coefficient can be represented by Eq. (5) [37]:

$$\Phi(x,t) = \frac{1}{k} \sqrt{4\alpha t} \left( \frac{1}{\sqrt{\pi}} exp\left( -\frac{1}{4Fo} \right) - \frac{1}{\sqrt{4Fo}} erfc\left( \frac{1}{\sqrt{4Fo}} \right) \right) \tag{5}$$

The important points which have been considered for estimating $\dot{q}(t)$ are enumerated below:

1. A functional form for $\dot{q}(t)$ is assumed for times $t_{\mathrm{M}}, t_{\mathrm{M+1}}, \ldots\ldots, t_{\mathrm{M+r-1}}$, where heat flux is known for $t < t_{\mathrm{M-1}}$.
2. The heat flux components are estimated for the assumed constant heat flux functional form.
3. Future temperatures points are used to account the delayed temperature response at an interior location.
4. $M$ is increased by 'one' and the procedure is repeated.
5. It is assumed that several future heat fluxes are constant with time.
6. To stabilize the IHCP algorithm the interfacial heat flux components $\dot{q}_M$, $\dot{q}_{M+1}$, ……, $\dot{q}_{M+r-1}$ are assumed to be equal and represented as:

$$\dot{q}_{M+1} = \dot{q}_{M+2} = \ldots\ldots = \dot{q}_{M+r-1} = \dot{q}_M \qquad (6)$$

Temperature extracted from the nodes $T_h$ and $T_c$ has been used in the estimation of transient heat flux, $\dot{q}(t)$. Subsequently, the estimated value of $\dot{q}(t)$ has been used to evaluate transient TCC, $h(t)$ by using Eq. (1).

### 3. Apparatus and instrumentation

Experiments have been performed in an updated version of uniquely designed set-up [4, 6] which was fabricated to carry out axial heat flow steady state experiments. Fig. 2 shows the schematic of complete experimental set-up indicating all the attachments along with the line diagram for three different configurations illustrating thermocouple positions. The complete details of apparatus and instrumentations have been described well in an earlier publication and can be referred further [4, 6]; however for sake of completeness, the salient details related to present transient and steady state measurement have been briefed in the following paragraphs.

The suitably modified setup has a provision to perform transient heat transfer experiments to implement inverse heat conduction methodology while using semi-infinite conduction formulation in the best possible manner. It consists of a mechanism to separately hold upper and lower specimens. For heating purpose, a cylindrical steel block in which five 150 W high performance cartridge heaters are inserted vertically and has been utilized in conjunction with a precise and stable PID controller. The cooling of the lower specimen has been attained by putting it into the thermal contact of a specially designed cooling block made up of copper. Chilled fluid consisting of a mixture of ethylene glycol and water (volume ratio of 40-60) coming out of a specially designed highly precise and stable PID controlled chiller has been re-circulated through this cooling block. To ensure one dimensional heat flow as well as to avoid heat losses, an insulation block (Isomag® 175, Spokane Valley, WA, USA) has been provided at the top of

heating block and at the bottom of cooling block, which is a magnesium silicate based product with an outstanding combination of high compressive strength and low thermal conductivity at temperatures up to 1000 degree C. In the heat flow column, all the interfaces except the test interface are pasted with a highly conductive silicone paste to reduce the contact resistance of the interfaces and to maximize the heat flow. To perform experiments under different contact pressure, a hydraulic jack arrangement has been fitted beneath the cooling block in combination with the pre-calibrated digital load cell. To maintain the required pressure of the hydraulic circuit, a diaphragm type accumulator along with a check valve has been installed as work holding devices. These two devices have not only minimized any fluctuations in the loading circuit but also ensured constant loading at the interface of two contacting solids during experimental run.

*3.1 Experimental specimen*

Stainless steel metal has been selected for all test specimens. Different sets of upper and lower specimen for flat-flat, cylinder-flat and cylinder-cylinder configurations are prepared by using CNC wire cut EDM machine. Highly precise machining has produced not only flat surfaces but also generated precise contour as required for curvilinear geometries. Temperatures at different axial locations have been measured by using fast response K-type ungrounded micro thermocouples (wire diameter = 0.1 mm) with sheath diameter of 0.5 mm, super accurate, super stable (Omegaclad ®). Thermocouples have been mounted at the axial locations inside the specimens. The thermocouples have been carefully inserted deep up to the centerline (11.25 mm deep) inside the EDM drilled holes, and to fix the thermocouples, a highly conducting paste has been filled in the holes. The temperature logging has been obtained by a National Instrument NI cDAQ-9178 data acquisition chassis with a NI-9213 module for thermocouple interfacing. The same experimental facility has been used for transient as well as steady state experiments. Thermal properties of specimens used are measured based on transient plane heat source (TPS) hot disk method and for this purpose TPS 2500S Thermal conductivity system has been used.

*3.2 Experimental procedure and conditions*

All the experiments have been executed under ambient condition. Experiments have been performed to record the actual temperature measurements during the transient and steady state run. One dimensional transient temperature data at single locations in both the specimens has been recorded with time and provided as an input to IHCP to estimate the interfacial heat flux with time. Initially, upper body is heated and lower body is cooled separately. After attaining the specified initial temperatures, heater and chiller have been switched off and then cold body is brought into contact with the fixed hot body and pressed together to a specified contact pressure, which ensembles the actual transient runs involved during many of the manufacturing processes in the best possible manner. Eventually, the temperature changes have been recorded from thermocouples mounted inside of each of the contacting specimens.

Evidently, the inverse scheme has been pre-tested with the simulated measurements, and several outcomes have been concluded well in the preceding section. However, when it comes to implement these outcomes of numerical analysis in the standardization of transient experiment with thermocouples (an intrusive approach), there exists certain issues which need to be addressed before the experiments. One of the biggest issues is to mount the thermocouples exactly or even very near to the interface. In the present investigation, the closest thermocouple from the interface is mounted 2.0 mm away from it in each of the hot and cold specimens, and therefore it carries inherent in-accuracy in the results as observed through the subsequent analysis. Eventually, transient temperature histories from both the thermocouples ( $T_h$ and $T_c$ ) have been used to evaluate $\Delta T(t)$ and $\dot{q}(t)$. Transient experiments have been conducted with preset initial temperature conditions, i.e. $140 \pm 0.5$ and $54 \pm 0.5$ °C of the hot and cold specimens, respectively. Eventually, unknown $h(t)$ has been determined by using Eq. (1). The temperature variation of the distant thermocouple (Fig. 9) from the interface at the non-contacting side has also been recorded simultaneously, which ensures the viability of the validation of semi-infinite solid assumption during each transient experimental run. Due to shorter duration of transient run, the present experimental methodology holds its relevance, even there does not exist continuous heat supply and loss to the specimen from the heater and chiller, respectively.

Once transient experiment has been completed, heater and chiller have been restarted and kept under running condition without disturbing the contact of specimens and loading condition, until the test column attains the steady state condition. The steady state is considered to be achieved; only when the temperature difference at each location is not more than 0.1 °C in 20 minutes. The value of steady state heat fluxes, $\dot{q}_1$ and $\dot{q}_2$ are measured from upper and lower specimen respectively, while using the classical Fourier's conduction law. The average of upper and lower heat fluxes of each specimen are taken as the measure of interfacial heat flux $\dot{q}$. Subsequently, the steady state interfacial temperature difference $\Delta T$ has been measured directly by the thermocouples mounted across the interface at 2 mm away from each of mating ends. It is important to highlight that in any typical steady state experiments for estimating TCC, temperature drop at the interface are generally evaluated by using linear extrapolation of the temperature profiles of each contacting body to the interface. However, in view of valid comparison with the transient results, the steady-state TCC calculation has also been made on the basis of interfacial temperature drop, while using the measurements from the thermocouples $T_h$ and $T_c$ as illustrated in Fig. 1(b), i.e. temperature drop across the interface without extrapolation, $h_{\Delta T\_\text{no extrp.}}$ is being used during TCC calculation.

Experiments are conducted on steel- steel contacts to study the effect of interface loading, and different types of contact configuration on the estimation of TCC. Bibliographical review illustrates that the TCC investigations with flat-flat configurations have been generally reported

against nominal contact pressure (MPa) as the functional parameters. However, present investigation also carries the experiment with curvilinear contact models, which produces line-contact at the interface; therefore it becomes difficult to represent the loading parameter in pressure unit for analysis. Henceforth, force unit (kN) is being used altogether to represent the loading parameters for all of the curvilinear contact configurations under consideration, which has been directly measured on the basis of pre-calibrated load cell mounted axially below the specimens.

In the present analysis, initially transient heat transfer experiments with flat-flat configuration has been performed at four set of different loading conditions, varying between 0.63 kN to 6.25 kN. Subsequently, the investigation with two set of different curvilinear contact models namely, cylinder-flat and cylinder-cylinder configuration has been performed under three set of similar loading conditions ( 0.60-6.35 kN ), and comparison has been performed with the help of few of representative results. It is important to highlight that, due to the complexities of different nature of contacts, it is extremely inevitable to exactly maintain the same axial loading output. Therefore, the reading of hydraulic gage pressure is set to be equal for each of the contact configuration under run, which is monitored throughout during each of the test run. Interestingly, a typical value of 1600 psi of hydraulic pump gage reading corresponds to 5.0 kN, 5.2 kN, and 5.0 kN for the flat-flat, cylinder-flat, and cylinder-cylinder configurations.

## 4. Results and discussion

The experimental results presented in this section have been obtained while using the IHCP, which require pre-assessment of various associated parameters and its effect on the accuracy in the estimation of TCC through experimental measurements. In this regard, the present investigation firstly deals with the numerical prediction of thermal contact conductance, while utilizing the simulated measuring parameters. Eventually, this numerical analysis provides the basis of judicious selection of various associated parameters, and help the analysis based upon the actual experimental measurements for predicting the TCC.

### *4.1 Numerical predictions*

Simulated temperature measurements at different nodal locations of hot and cold bodies have been obtained from the solution of the direct problem by applying the suitable boundary conditions in Eq. (2), and the results for the duration of 100 seconds are shown in Fig. 3. Eventually, transient temperature data of respective nodes has been used for the estimation of $\dot{q}_{\text{est}}(t)$, and $\Delta T_{\text{est}}(t)$. The simulated temperature variation of the nodes close and far away from the interface, 2.0 and 28.5 mm, respectively has been used to get an estimate about the validity of semi-infinite assumption (Fig. 3). Assuming, the criteria of 1% temperature variation as the permissible limit, the simulated temperature variation graph (Fig. 3) clearly illustrate the viability of the present formulation up to 32 seconds as the minimum allowable time span. The inverse

algorithm has been solved by allowing simulated temperatures to match with the corresponding calculated temperatures in an exact manner. This exact matching of temperatures is known as Stoltz method [38] which corresponds to single future time step ($r = 1$), and it happens to be extremely sensitive to the measurement errors. To reduce the sensitivity dependence on measurement errors, more than one future time steps have been used and its influence on the estimated heat flux is shown in Fig. 4. It clearly illustrates the improvements in estimated values of interfacial heat flux, while increasing future time steps 2 to 4. In the present study, 4 future time steps have been used altogether for estimating interfacial heat flux.

It is well documented that the temperature response deep inside a semi-infinite body is lagged with respect to the heat flux excitation [26, 27] and becomes less pronounced for sensor located far away from the source of excitation. Since the accuracy of inverse solution (cause) is greatly influenced by the correctness of temperature measurements (effect), it is essentially desired to place the sensor closer to the interface for the correct estimation of interfacial heat flux. However, inserting the thermocouple apparently near the interface might be restrictive, hence may affect the correct estimate of heat flux. Therefore it is important to know in advance that, how far the sensor can be placed from the interface to get reasonably correct estimate of interfacial heat flux. Based upon the IHCP solution, present numerical analysis has been used to get an estimate about the permissible depth of sensor location from the interface, without compromising much in the interfacial heat flux prediction while using a single thermocouple measurement. Simulated temperature data of different nodal locations (different values of $x_1$) have been used in estimating the interfacial heat flux. Eventually, the variation of heat flux estimate is shown with different values of $x_1$, i.e. 0.5, 1.0, 1.5, 2.0 and 5.0 mm in Fig. 5. It has been observed that nature of all the curves remain exactly same and stable, except the curves representing the thermocouple location at $x_1 = 5.0$ mm, however their maximum heat flux are slightly higher than the each of the preceding locations. It has been concluded that, as locations of sensor moves further away from the interface, i.e. $x_1 \geq 5.0$ mm, the nature of heat flux characteristic starts deviating significantly at the onset of heat transfer process.

The next parameter which has been tested to check its influence on the estimation of TCC is the size of time step ($\Delta t$). The variation of numerically estimated TCC i.e. $h_{\text{est}}(t)$ has been shown for different values of $\Delta t$, i.e. 0.05, 0.1, 0.5, 1.0, 2.0, and 4.0 s in Fig. 6. The smallest time step, $\Delta t = 0.05$ s produces a very unstable value of $h_{est}(t)$, and hence does not convey right information about the correct estimate of TCC. Increasing the time steps produces a stable outcome, however it results in with the significant over-prediction in the estimate of TCC against the supplied result. Evidently up to 40 s, $\Delta t = 0.1$ s gives the reasonably correct and stable information about the TCC, which optimally matches all along with the supplied value of TCC used in direct problem based solution. Therefore based upon the present numerical outcome, $\Delta t$

= 0.1 s has been suitably recommended as the most appropriate time step for the prediction of TCC.

At this stage, it is important to highlight that the ratio of the heat flux transient, $\dot{q}(t)$ and the interfacial temperature drop variation over the interface, $\Delta T_{\text{est}}(t)$ is used to estimate the TCC, which might bring further proneness to error towards predicting the TCC. Therefore, even though the result shows (Fig. 5) the insignificant effect of thermal lagging on the estimate of heat flux due to the change in sensor location (in the near vicinity of contact, $x_1 < 5.0$ mm); it is essentially required to examine the effect of sensor location on TCC, which inherently affect $\Delta T_{\text{est}}(t)$ in an indirect manner. Here, five different values of $\Delta T_{\text{est}}(t)$ have been used for the determination of $h_{\text{est}}(t)$ by calculating temperature difference at different locations from both the bodies, *i.e.* 0.0 (exactly at the interface), 0.5, 1.0, 1.5, and 2.0 mm from the interface. Eventually, $h_{\text{est}}(t)$ is obtained by substituting the respective values of $\Delta T_{\text{est}}(t)$ along with $\dot{q}_{\text{est}}(t)$ in Eq. (1). The results have been shown in Fig. 7. It is observed, that the estimated TCC matches perfectly with $h_{\text{sup}}$, only when $\Delta T_{\text{est}}(t)$ has been evaluated on the basis of temperature difference exactly at the interfacial nodes. Moreover, exact matching of TCC has been observed up to 32-40 seconds, which falls in tune with allowable time span criteria for the pre-assumption of semi-infinite body. An under-prediction of the 12-35% in the TCC can be observed, while sensor location varies from 0.5 to 2.0 mm away from the interface. Interestingly, the value of estimated TCC remains almost constant up to the total duration of 40 s, indicating the viability of the results based upon the present conduction modelling. It is worthy enough to mention that after achieving the constant steady value (~ up to 40 s); the value of estimated TCC veered away from the actually supplied value $h_{\text{sup}}$ for all of the cases, which should be considered superficial due to the limiting criteria about the validity of semi-infinite solid assumption (as discussed earlier).

Conclusively, these outcomes based upon the numerically generated measurements are quite important and provide valuable input about the possible error in the TCC estimation based upon the actual experimental feasibility constraints. Additionally, it provides a rationale estimate about the accuracy in the estimation of TCC using sensors exactly at the interface, which is practically inevitable to evade in actual experiments.

*4.2 Experimental estimation*

Primarily, the focus of the present analysis is to estimate the transient variation of TCC at the onset of heat flow establishment between the pressed thermal contacts of flat-flat and curvilinear contacts under different axial loading conditions. Subsequently, the analysis has been extended to compare the transient TCC with that of the steady-state based TCC estimation for each set of geometrical configurations under consideration, and evolve the suitable strategy to

correctly predict the steady-state TCC estimate with the help of transient approach. To the best of our knowledge, the transient TCC variation between the curvilinear contacts under consideration has not been found in the pertinent literature, and even the very limited set of steady-state experiments were performed with the curvilinear contact models [5, 14], and therefore a valid comparison of the curvilinear contact results from the available literature is not feasible. Therefore, as a standardization exercise of the present set-up, methodology and the measurement, the steady state experimental results of flat-flat contact have been compared well with the published literatures [2, 6, 39]. Subsequently, the investigation with two set of different curvilinear contact models namely, cylinder-flat and cylinder-cylinder configuration has been performed under three set of similar loading conditions ( 0.60-6.30 kN ), and some of the typical results have been presented suitably to get the valuable insight about the effect of nature of contact on the transient TCC. Eventually, a strategy has been proposed for the selection of representative value of TCC to get the steady state TCC from the instantaneous TCC variation curve with time.

*4.2.1 Comparison of flat-flat TCC results with published correlations*

Several theoretical models exists in the pertinent literature, which were proposed to estimate the TCC depending upon the nature of deformation of the contacting asperities. In this regard, Mikic [2] had linked the modulus of elasticity as the significant factor, which plays a major role for the case of elastic deformation, and reported that deformation would be mainly elastic for $(H/E'm_{\text{eff}}) \geq 3$ and plastic for $(H/E'm_{\text{eff}}) \leq 1/3$. Based upon the Mikic [2] plasticity index, present test surfaces of flat-flat contact combinations are supposed to exhibit plastic deformation. Therefore, the present experimental steady state TCC estimate of flat-flat contact has been compared with some of the available plastic contact models [2, 39]. Furthermore, the results were also compared against the published correlations developed on the basis of experimental investigations. Fig. 8 shows the comparison of steady state TCC obtained from flat-flat contact with the published literature [2,6,39], where the experimental TCC and interfacial pressure have been suitably non-dimentionalized on the basis of related parameters as given in Table 2. The correlations used for present comparison are also enumerated here in Table 3. Evidently, most of the experimental results lie between the two bounds set by the theoretical and experimental based correlations. The nature of present disagreement can be linked with the uncertainty associated with the selection of correct exponent of correlations, which are quite coherent with the findings of other researchers [4, 6, 16, 41].

*4.2.2 Transient Temperature*

As discussed earlier, the transient inverse analysis is based upon the 1-D conduction solution of semi-infinite solid substrate. Therefore, the temperature variation with time at different locations (Fig. 9) along and away from the interface has been recorded for each set of experiments, which ensures the experimental validation of semi-infinite solid assumption during

any transient run. A typical result from each set of contact configuration at the similar loading condition (□5.0 kN) has been shown in Fig. 9. The temperature histories show the ability of ultra-sensitive micro-thermocouples sensors to record high quality temperature measurements. It has been observed that heat flow get initiated from hot to cold bodies, immediately after the contact, and a sharp temperature variation in the interfacial thermocouple of both the bodies ($T_h$, and $T_c$) happens immediately at the onset of contact. The temperature varies exponentially and the gradient of the temperature curve stabilizes shortly for flat-flat contact as against the curvilinear contacts, which can be explained on the basis of limited scope of contact area of curvilinear models through which the heat flow occurs. Evidently, temperatures of farthest nodes from the interface attains its 1% change at around 32.0-40 seconds for flat-flat contact configurations, whereas it is quite delayed for cylinder-flat, and cylinder-cylinder contact models under the similar loading and thermal conditions. The results from the curvilinear contact configuration illustrates that the temperature change of the farthest sensor becomes evident only after 70 to 80 seconds, which can be attributed to the beginning of surface heat transfer penetration to the interior locations in both the bodies. These temperature curves substantiate the scope of the 1-D semi-infinite solid assumption for each configuration, and provide the allowable time duration which forms the basis of present analysis towards experimental estimation of $\dot{q}(t)$ by using Eq. (4).

*4.2.3 Transient Heat Flux*

The instantaneous heat flux variation with time has been estimated for flat-flat, cylinder-flat and cylinder-cylinder contacts under axial loading conditions. These results are obtained on the basis of inverse modelling while using the 1-D semi-infinite conduction solution, whose validity is inherently restricted due to limiting criteria of the penetration time [36]. Therefore results are suitably shown only for a shorter durations (up to 40 sec) as against the interfacial temperature drop variation inferred on the basis of $T_h$ and $T_c$ variation as depicted in Fig. 9. It is important to mention that the results would be superficial beyond the allowable time constraints ($\approx$ 40 sec in general), afterward it fails to satisfy the permissible penetration time criteria about the validity of semi-infinite solid assumption, hence has not been taken into consideration during transient heat flux representations (Fig. 10, and Fig. 11). Inherently, TCC at the interface does not depend only on the heat flux density across the interface, it get affected by the interfacial temperature drop as well, therefore the variation of interfacial temperature drop inferred on the basis of difference between $T_h$ and $T_c$ is also shown all along the heat flux transient during each set of experiments.

Firstly the transient heat flux outcome for the flat-flat contacts under four different loading conditions are shown in Fig. 10, where the heat flux estimate obtained on the basis of upper hot specimen, lower cold specimen, and the average of the duo have been shown together. In a way, the average of heat fluxes is generally regarded as the effective heat flux passing through the interface, henceforth only the average heat flux values, $\dot{q}(t)$ are used for subsequent TCC

analysis. Evidently, the heat flux transient illustrated in Fig. 10 shows a clear peak for all the loading conditions representing a maximum value of heat fluxes, which is attained shortly (up to 4-6 seconds) after the contact of both the bodies. Most of the previous works related with the various manufacturing processes had shown the same trend [28-31], where sharp rise in the heat flux were linked with the high heat addition due to the good contact at the onset of various manufacturing processes. Herein the peak heat flux value increases with the increase in the loads, and this can be attributed to the respective rise in the quantum of the driving force for the heat transfer due to the various associated factors. Presently, the initial driving force for heat transfer get accelerated due to the greater temperature difference across the interface, as well as due to the increase in the interfacial pressures resulting good contact (i.e. reduced contact resistances) at the interface. Evidently during the onset of contact process the temperature difference across the interface happens to be the most due to the initial conditions of the hot and cold block. Further, the application of axial load affects the deformation of the contact asperities causing growth in the real contact area, resulting better contact. Consequentially, both of these factor act favourably to accelerate the initial driving force and result in terms of sharp rise in heat flux up to a peak value. Certainly, the deformations in the asperities might stabilizes early as against the temperature differences, which remains the only dominant factor to drive the heat flow until the blocks attain the thermally steady state condition. Recent study [23], shows a direct link between the applied force variation with that of the contact heat transfer coefficient and illustrated, that the temporal profile of the temperature exhibit less effect as against the load transient. Correlating this mechanism with the heat flux transient, the time of occurrence of $q_{\max}$ can be regarded as the completion of the asperities deformation due to the application of sudden contact, after which the temperature difference across the interface remains the only factor which might contribute to drive the heat flow further.

Fig. 10 also illustrates that the temperature difference across the interface decreases exponentially, and henceforth a significant decrease in the driving force of heat transfer is inevitable beyond the occurrence of $q_{\max}$, which reflects consequential decay in the heat flux transient. An important observation from the above experimental results are that, as the load gets increased, not only the maximum value of $\dot{q}_{\mathrm{c}}(t)$ and $\dot{q}_{\mathrm{h}}(t)$ has been increased but these two also gets very close to the average heat flux, $\dot{q}(t)$. Evidently, mismatch in heat flux estimation between the upper and lower specimen's results shows a diminishing trend at higher loadings conditions; indicating the reduction in heat losses from contacting bodies. Interestingly once the heat flux attains the peak value, the gradient of the heat flux transient varies along with the interfacial temperature drop gradient, and afterward both the transient curve moves in tandem indicating a quasi-static equilibrium of heat flow up to the total time span under consideration. Invariably, these results provides the valuable insight about the present methodology in successfully estimating the variation of TCC at the onset of contact followed by the comparison with the steady state heat TCC experiments.

Subsequently, the present approach is implemented for different curvilinear contact configurations under consideration. Eventually, Fig. 11 shows the transient heat flux estimates obtained from the upper hot specimen, lower cold specimen, and the average of the both for cylinder-flat and cylinder-cylinder line contacts along with their respective interfacial temperature drop variation at a typical loading condition (□5.0±0.2 kN). Here again the heat flux transient showed a clear peak for both of the cases, which is attained shortly after the contact and also represents the maximum value of heat flux during the total duration of analysis. Furthermore, the time of occurrence of $q_{max}$ is found to be of the same order (up to 4 sec) as against the respective flat-flat transient run. Whereas, contrary to the earlier results (Fig. 10) of flat-flat surface contact models under similar axial load (5.0 kN), there exists a greater degree of mismatch in the heat flux curves and its peak values for both of the hot and cold bodies during the onset of the each contact. Kumar et al. [13] had observed that the heat flow across the curvilinear contact joints was additionally constrained at macro level through the contour zones corresponding to macro constrictions from curved surfaces. Classical Hertz theory [42] explains that any typical curvilinear contact can be represented by a narrow rectangular strip, which exhibits the area contours around mating curvatures, whose size is directly influenced by the loading conditions, and the curvature of the mating surface as well. Evidently, under the similar loading condition, area contour of the cylinder-cylinder contact model is expected to be less than that of the cylinder-flat contact model, followed by the flat-flat surface contact area. Henceforth, in addition to the micro surface constriction resistances, there exists an additional scope of macroscopic contact resistance due to these circumscribed area contours, resulting consequential increase in the overall contact resistance which restricts the heat flow at the interface. This explains well about the relatively lesser magnitude of overall heat flux magnitude and the significant heat loss from upper specimen to the lower specimen through these curvilinear contact combinations.

Consequentially, Fig. 11 illustrates the instantaneous variation of interfacial temperature drop which act as the sole driving factor of heat flow even after heat flux transient attains a peak. The value of interfacial temperature is high at the onset of contact, and decays gradually at lesser rate as against the flat-flat configuration. Evidently, the decrease in the value of instantaneous interfacial temperature drop act as the prime reason for the decrease in the heat flux transient after the peak during the whole span of test run. Here, an important deviation in the variation of interfacial temperature drop has been observed as against the flat-flat contact configuration, i.e. the retarded rate of instantaneous temperature drop variation has been observed as against the transient heat flux variation. Basically, the gradient of the heat flux transient does not vary along the interfacial temperature drop gradient during initial stage after the contact. Both of these curves moves in-tandem with fixed offset quite late (beyond two third of the total duration under representation (40 sec), i.e. equivalent to ~27 sec); only then it appears in a quasi-static equilibrium of heat flow condition during the remaining span of time (40 sec), which is the

permissible duration of span towards the viability of the present 1-D semi-infinite conduction solution. This results is quite contrary to the earlier observations found during the transient inverse analysis related with the conforming type of flat-flat surface contact models, and hence may carry severe implications on extracting the steady state TCC by present transient analysis. The reason for this delayed attainment of quasi-static equilibrium in heat flow can be primarily attributed toward the non-conforming nature of mating surfaces leading to circumscribed area contours in the form of typical line contact models, which act as the restricting passage for the heat lines during the initiations of the heat flow. It appears that the constriction in the heat flow through the line in contact, allows to contract and then expand the heat line immediately at the onset of contact leading to deviation from the pre-assumed 1-D axial heat transfer. Lately, these heat lines get stabilizes and follows the typical behaviour 1-D axial heat flow through each of the specimens, and hence helps in attaining the quasi-static equilibrium state of heat flow.

*4.2.4 Transient thermal contact conductance (TCC)*

The instantaneous estimate of TCC variation with time has been evaluated for flat-flat, cylinder-flat and cylinder-cylinder contacts under various axial loading conditions. Firstly, the results for the flat-flat configurations have been presented separately along with the steady state TCC estimate. Later, the transient TCC results related with the two of the non-conforming type of curvilinear contacts configurations, namely cylinder-flat and cylinder-cylinder combinations has been presented together with the transient TCC of flat-flat, and changing nature of variation in instantaneous TCC , $h(t)$ has been documented. Finally, the effect of loading condition on different contact configuration under consideration has been quantified, while each of the results has been compared together.

*4.2.4.1 Conforming flat-flat contacts*

The variation of TCC with time for the flat-flat configuration under four different loading conditions (0.63, 3.35, 5.00, and 6.25 kN ) is shown in Fig. 12, where transient TCC, $h(t)$ has been obtained by using Eq. (1) with a modification that the numerator and denominator represents instantaneous value of $\dot{q}(t)$ and $\Delta T(t)$ under respective loading conditions. The calculated $h(t)$ increases rapidly and attains a steady value shortly onward to the time of occurrence of $q_{\max}$, then stabilizes soon with very little variation. Evidently, during the present scope of time span (40 sec), the experimentally estimated instantaneous TCC, $h(t)$ follows the similar trend of TCC variation (Fig. 7), as obtained earlier on the basis of simulated measurements (section 4.1). However there exists a remarkable discrepancy with that of the numerical outcome, which exists in terms of the immediate attainment of the peak/steady value of TCC. This can be easily explained on the basis of actual experimental lag which might exists while bringing the actual physical contact of the specimens and consequential initiations of the heat flow and is evitable during numerical analysis.

All of the curves in Fig. 12 show the rapid rise in TCC value immediately at the onset of contact, and thus follows the similar trends as found in the transient heat flux curves (Fig. 10), and henceforth it can be attributed again to the enhanced capacity of heat transfer between the test surfaces due to the rapid decrease in the interfacial temperature drops. As discussed in the preceding section (section 4.2.3) that once the interfacial load reaches the prescribed value, the interfacial temperature drop and heat flux decreases gradually and afterward each curve attains a similar degree of gradient with time and moves in tandem with a fixed offset, and heat flow appears to be under quasi-static thermal equilibrium condition. Therefore the TCC, which inherently represents the ratios of the transient heat flux and the interfacial temperature drop variation with time, becomes quite steady against a fixed value of TCC during the quasi-static state of thermal equilibrium. Further, the effect of the increase in axial load at the interface is observed in terms of the increase in the fixed offset value between the transient heat flux and the instantaneous interfacial temperature drop, which resulted in terms of the matching enhancement in the TCC magnitude.

*4.2.4.2 Non-conforming curvilinear contacts*

Figure 13 shows the instantaneous estimate of TCC variation of both the non-conforming type of curvilinear contacts configurations, namely cylinder-flat and cylinder-cylinder combinations under three typical axial loading condition ranging between  6.0-6.25 kN. TCC variation with time for the conforming flat-flat contact configuration under similar axial loading conditions have also been superimposed over each of the graphs for ease of comparison, which clearly illustrates that the nature of TCC variation for the curvilinear contact combinations are quite different with the flat-flat contact configurations. Each $h(t)$ results of curvilinear contact combination exhibit a clear dominant peak, which is attained shortly within half of the span corresponding to the peak value of TCC for the flat-flat configuration. Once the peak in TCC has been attained during the curvilinear contact models, it decreases gradually and attains a steady and stable value quite late as against the transient TCC of flat-flat, where it get stabilized quickly and even does not carry a sharp peak with an exponential decay in $h(t)$. However, in both of the curvilinear contact configurations, the transient TCC, $h(t)$ attains a steady and stable value during the period which carries the quasi-static equilibrium of heat flow as observed in transient heat flux curves (Fig. 11)..

Additionally, as a comparison with the steady-state TCC value under equivalent axial loading conditions, which is being evaluated on the basis of direct temperature drop measurements while using the interfacial thermocouples $T_{\mathrm{h}}$ and $T_{\mathrm{c}}$, the constant value of $h_{\Delta \mathrm{T\_no\ extrp.}}$ is also superimposed over the respective transient TCC plots as a straight line in these graphs (Fig. 13). It is important to mention that the each of the straight line simply indicates the

steady-state TCC, $h_{\Delta T\_no\ extrp.}$ based upon the temperature drop measurement across the interface without extrapolation, and it should not be treated as the variation of TCC along the time axis. Through these plots, it is also evident that in each of the cases the transient TCC $h(t)$ get stabilizes along $h_{\Delta T\_no\ extrp.}$ with very little deviation. This agreement of transient TCC $h(t)$ with that of steady state TCC $h_{\Delta T\_no\ extrp.}$ provides a valuable insight.

Evidently, the instantaneous TCC variation of flat-flat and the curvilinear configuration illustrates that the agreement between the transient TCC $h(t)$ with that of steady state TCC $h_{\Delta T\_no\ extrp.}$ is observed, only when it attains the quasi-static kind of equilibrium, as observed in the preceding plots (Fig. 10 and Fig. 11). It is important to assert that, the quasi-static equilibrium state of heat flow condition has been observed shortly within overall span of allowable penetration time [24] of the substrate for the conforming type of flat-flat contact model. Whereas, con-conforming type of curvilinear contact experiment had already shown a different behaviour of transient heat flux against the interfacial temperature drop variation (Fig 11), henceforth a steady and stable value of $h(t)$ from the onset of $q_{\max}$ appears to be quite unlikely, and delays the agreement with $h_{\Delta T\_no\ extrp.}$.

Apart from the nature of the transient TCC in curvilinear contacts, Fig. 13 also represents the effect of loading on the transient TCC. For the same level of increment in load $\sim 0.60$ to $5.20$ kN in both the contacts, maximum increase in TCC is observed for cylinder-flat as against cylinder-cylinder contact. This finding supports the previous discussion on the transient heat flux of cylinder-flat and cylinder-cylinder contacts where it has been explained that under similar loading condition, area contour of the cylinder-cylinder contact is expected to be less than that of the cylinder-flat contact. Afterwards further increase in loading ($\sim 5.00$ to $6.25$ kN) shows proportionate rise in the TCC magnitude in each of curvilinear contact configurations.

*4.2.5 Steady state versus transient TCC: A comparative assessment*

At this stage, it would be interesting to highlight the concern raised earlier (Section 1) regarding the selection of representative value of TCC to get the steady state TCC from the instantaneous TCC variation curve with time, especially in the context of predicting the steady state TCC estimate on the basis of transient measurement of temperature values. In this regard, it becomes inevitable to compare the present transient results with the corresponding steady state measurements, which are generally well acceptable as a reliable approach for estimating the TCC for specimen under consistently pressed contact condition. As discussed earlier (at the end of preceding section 3.2), present transient TCC estimate is entirely based upon the actual thermocouple's measurement which lies at 2 mm away from the mating end; henceforth steady state TCC estimate has also been evaluated directly on the basis of steady state interfacial

temperature drop ($\Delta T$) measurements (i.e. without extrapolation), and the results of each set of experiments ($h_{\Delta T\_\text{no exptrp}}$) have been shown together by a straight dotted line on the respective graphs (Fig. 12, and 13) for the comparison. On the basis of these graphical comparisons, it can be inferred that the value of instantaneous/transient TCC which corresponds to the peak zone of transient heat flux i.e. $q_{\max}$ cannot be regarded as the representative value of the TCC. Instead, it will be reasonable to conclude that once the instantaneous TCC value get stabilized during the typical quasi-static equilibrium state of heat flow, it matches remarkably well with the steady state TCC values. Evidently, the match of the stabilized steady value of Transient TCC with the steady state TCC, $h_{\Delta T\_\text{no exptrp}}$ occur quite late during the non-conforming kind of curvilinear contact configurations as against the flat-flat case which is well within expectation on the basis of respective transient heat flux and instantaneous interfacial temperature drop variations.

Based upon these observations, it can be concluded that the quasi-steady state condition of the transient heat flow is successfully able to extract the steady-state TCC measurement with greater reliability. This can be treated as an important observation, and provides a plausible solution to predict the steady state TCC measurement on the basis of short duration based transient experiments. Contrary to the earlier experiments with flat-flat contact configurations [16, 23, 32, and 34] where tremendous ambiguity exists during the selection of representative value from the instantaneous TCC curve, present transient methodology provides a reliable outcome to correlate the transient TCC measurement with that of the steady state TCC value on the basis of simple 1-D solution of semi-infinite conduction problem.

Lastly, comparison of stabilized value of $h(t)$ with the standard steady state TCC evaluated on the basis of linear extrapolation of the temperature profiles, i.e. $h_{\Delta\text{T\_extrp.}}$ has been made to quantify the in-evitable range of under prediction during present experiments due to the practically possible location of the thermocouple in each of the specimens, and results are shown in Table 4. It has been observed that the steady value of instantaneous TCC $h(t)$, which inherently represent the quasi-steady state heat flow condition during any transient run, does a not match well with $h_{\Delta\text{T\_extrp.}}$. The transient results show an under prediction of the steady state TCC value ($h_{\Delta\text{T\_extrp.}}$) in the range of 30 to 60 % for flat-flat contact, while load varies in between 0.63 kN to 6.25 kN, respectively. This is quite understandable, and larger under prediction in the results at higher loading condition can be attributed toward the increase in uncertainty of TCC estimate at higher loading conditions due to greater extrapolation errors, and other associated factors [4]. Furthermore, the under prediction of the steady state TCC at the nominal loading condition (0.63 kN) falls in tune with the numerical prediction illustrated in Fig. 7, while compared with the results for the similar sensor location case. In this study, the nearest temperature sensors are inserted at around 2.0 mm away from the interface due to various

practical constraints, therefore an under prediction of the order of ~ 30-35% with the steady state TCC value is quite understandable.

The comparison chart (Table 4) for the curvilinear contacts shows an interesting outcome with drastic reduction in the under prediction of steady state TCC by transient results. In comparison to the flat-flat configuration at highest loading condition, the under prediction reduces from 60 % to 7.98, and 6.64 for the cylinder-flat and cylinder-cylinder contacts, respectively. The reason for the same can be attributed to the increase in the degree of heat losses between the upper and the lower specimen for curvilinear contacts against flat-flat contact. Conclusively, the above results prove the credibility of the present methodology to get the accurate estimation of steady state TCC with short duration transient experiments. It is also well understood that the under prediction of steady state TCC is not due to the inability of the algorithm, rather due to the physical and practical limitation of sensors placement at the interface for the calculation of $\Delta T(t)$. Therefore, present methodology looks quite promising when used in conjunction with the modern high resolution optical based temperature mapping tools, which can correctly predict the temperature in the immediate vicinity of the interface, and therefore would be the scope of our upcoming research investigations in detail.

## 5. Uncertainty analysis

The uncertainty of an entity depends on several independent variables. Uncertainty in estimating temperature jump for contacts of flat-flat, cylinder-flat and cylinder-cylinder are $\pm 7.22$, $\pm 2.00$ and $\pm 2.01$ % respectively. Accuracy in the heat flux calculation from specimens depends on the thermal conductivity of specimens. Uncertainty in the measurement of thermal conductivity of specimens is $\pm 1.50$ %. The maximum heat flux difference through test specimens for the contact of flat-flat, cylinder-flat and cylinder-cylinder have been estimated as $\pm 10.50$ %, $\pm 18.40$ % and $\pm 19.80$ %, respectively. Finally, based on the law of error propagation model by Holman [43], the overall uncertainty in experimental TCC for contacts of flat-flat, cylinder-flat and cylinder-cylinder have been estimated as $\pm 14.37$, $\pm 19.61$ and $\pm 20.97$ % respectively.

## 6. Conclusions

A single sensor based inverse algorithm has been explored for the estimation of TCC between different contact configurations while using 1-D semi-infinite conduction solution. The inverse problem is solved by the sequential estimation method considering future time steps. Firstly, the methodology has been tested successfully with the numerically generated temperature results, and the effect of varying time steps (0.05-4.0 sec) and sensor location from the interface (0.5-5.0 mm) have been illustrated. It has been observed that estimate of interfacial heat flux is negligibly effected, if nodal location of the sensor is well within 6-7% of the length of body from the

interface; however it carries significant effect on the TCC values. An under prediction of TCC value in the order of 12-35% has been obtained, while sensor location varies from 0.5 to 2.0 mm away from the interface. Primarily, the numerical analysis provides a rationale estimate about the accuracy in the sequential estimation based TCC evaluation while using intrusive sensors away from the interface, which is practically inevitable to evade in actual experiments.

Later, experiments have been performed in a uniquely designed setup. As standardization of the present set-up, methodology and the measurement, the steady state experimental results of flat-flat contact have been compared with the published literatures, and consequently the detailed comparison between transient and steady state results has been performed for flat-flat, cylinder-flat, and cylinder-cylinder contact configurations under various loading conditions. Primary results of transient heat flux showed a clear peak for each of the contact combinations, which has been attained shortly after the contact and also represents the maximum value of heat flux during the total duration of analysis. The transient heat flux has shown an exponential decay after the peak, and the decrease in the instantaneous interfacial temperature drop value has been concluded as the prime reason for this gradual decay. The gradient of the heat flux transient has been found to vary along with the interfacial temperature drop gradient after suitable span of time, and afterward both the transient curve moves in tandem indicating a quasi-static equilibrium of heat flow. Conforming type of flat-flat contact attained the quasi-static equilibrium shortly after the occurrence of $q_{\max}$, whereas it gets delayed for the curvilinear contact experiments. Consequential curve of the transient TCC illustrated that the instantaneous TCC value get stabilized only during the typical quasi-static equilibrium state of heat flow, and this value of TCC matches remarkably well with the steady state TCC values obtained on the basis of direct steady state interfacial temperature drop measurements. It has been shown that the quasi-steady state condition of the transient heat flow is successful in evaluating the steady-state TCC measurement with greater reliability. This can be treated as an important observation, and provides a plausible solution to predict the steady state TCC measurement on the basis of short duration transient experiments.

Finally, a comparison of stabilized value of $h(t)$ with the steady state TCC evaluated on the basis of linear extrapolation of the temperature profiles, i.e. $h_{\Delta T\_extrp.}$ has been made, and range of under-prediction in the steady state TCC for each of the contact configurations have been quantified. For sure, it advocates towards the implementation of the non-intrusive based optical techniques; however seeing the ease in implementation and associated cost of the experiment, present investigations with thermocouple can be regarded as the baseline experiment which provide valuable comparison between the transient and steady state results, and deals about the suitability of the present experimental methodology for the estimation of TCC between various contact configurations.

**Acknowledgements**

The authors gratefully acknowledge the financial support of the Bhabha Atomic Research Centre (BARC), India for initiating this research activity in Mechanical & Industrial Engineering Department (MIED) at Indian Institute of Technology (IIT) Roorkee, India. Special gratitude to Dr Deb Mukhopadhyay, Sc 'H' BARC, India for motivation and developing interest in the area of 'thermal contact conductance'.

**Nomenclature**

| | |
|---|---|
| $E$ | modulus of elasticity |
| $E'$ | reduced modulus of elasticity, $E' = \left[\left((1-\nu_1^2)/E_1\right)+\left((1-\nu_2^2)/E_2\right)\right]^{-1}$ |
| $Fo$ | Fourier number |
| $H$ | Vickers hardness |
| $h$ | interfacial heat transfer co-efficient or TCC, W/m$^2$K |
| $h^*$ | nondimensional TCC, $h^* = (hm_{\text{eff}})/(\sigma_{\text{eff}} k_{\text{eff}})$ |
| $k$ | thermal conductivity, W/m K |
| $k_{\text{eff}}$ | effective thermal conductivity, $k_{\text{eff}} = \sqrt{(k_1^2 + k_2^2)}$ |
| $L$ | length of a body, m |
| $M$ | general time step index |
| $m$ | rms roughness |
| $m_{\text{eff}}$ | effective rms roughness $m_{\text{eff}} = \sqrt{(m_1^2 + m_2^2)}$ |
| $P$ | interfacial pressure for flat-flat contact, MPa |
| $P^*$ | nondimensional pressure, $P^* = P/H$ |
| $\dot{q}$ | average interfacial heat flux, W/m$^2$ |

| | |
|---|---|
| $r$ | future time steps or number of future temperatures |
| $t$ | time, s |
| $T$ | temperature, ℃ |
| $\hat{T}$ | calculated temperature, K |
| $x$ | spatial coordinate, m |
| $x_1$ | distance between interface and sensor position in semi-infinite bodies |
| $Y$ | measured temperature, K |

Greek Symbols

| | |
|---|---|
| $\Delta T$ | temperature drop at the interface, ℃ |
| $\alpha$ | thermal diffusivity, $m^2/s$ |
| $\sigma$ | arithmetic roughness slope |
| $\sigma_{eff}$ | effective arithmetic roughness slope, $\sigma_{eff} = \sqrt{(\sigma_1^2 + \sigma_2^2)}$ |
| $\Phi$ | sensitivity coefficient, $m^2K/W$ |
| $\nu$ | Poissson's ratio |
| $\Delta t$ | time step size, s |

Subscripts

| | |
|---|---|
| *extrp.* | extrapolation, $\Delta T$ calculated at the interface |

| | |
|---|---|
| *no extrp.* | no extrapolation, $\Delta T$ calculated at the nearest sensor from the interface |
| $h$ | hot |
| $c$ | cold |
| $1, 2$ | lower body, upper body |
| *sup* | supplied data |
| $i$ | Initial |
| *est* | estimated (from numerical data) |
| *max* | maximum |

**References**


[1] M.G. Cooper, B.B. Mikic, M.M. Yovanovich, Thermal contact conductance, Int. J. Heat Mass Transf. 12 (1969) 279–300.

[2] B.B. Mikic, Thermal contact conductance; theoretical considerations, Int. J. Heat Mass Transf. 17 (1974) 205–214.

[3] P. Sadowski, S. Stupkiewicz, A model of thermal contact conductance at high real contact area fractions, Wear 268 (2010) 77–85.

[4] A. Tariq, M. Asif, Experimental investigation of thermal contact conductance for nominally flat metallic contact, Heat Mass Transf. 52 (2016) 291–307.

[5] S. Kumar, A. Tariq, Steady state experimental investigation of thermal contact conductance between curvilinear contacts using Liquid Crystal Thermography, Int. J. Therm. Sci. 118 (2017) 53–68.

[6] M. Asif, A. Tariq, Correlations of thermal contact conductance for nominally flat metallic contact in vacuum, Exp. Heat Transf. 6152 (2016) 1–29.

[7] Misra, P., Nagaraju, J., An experimental study to show the effect of thermal stress on thermal contact conductance at sub-megapascal contact pressures. *Journal of Heat Transfer*, 132(9) (2010) 94501.

[8] Ding, C., Wang, R. Thermal contact conductance of stainless steel-GFRP interface under vacuum environment, Experimental Thermal and Fluid Science, 42 (2012) 1–5.

[9] Zhu, Z., Zhang, L.W., Wu, Q.K., Gu, S.D., An experimental investigation of thermal contact conductance of Hastelloy C-276 based on steady-state heat flux method. International Communications in Heat and Mass Transfer, 41 (2013) 63–67.

[10] Sponagle, B., Groulx, D., Measurement of thermal interface conductance at variable clamping pressures using a steady state method, Applied Thermal Engineering, 96 (2016) 671–681.

[11] G.H. Ayers, Cylindrical thermal contact conductance, M.S. Thesis, Texas A&M University, Texas, 2003.

[12] C.V. Madhusudana, Thermal conductance of cylindrical joints, Int. J Heat Mass Transf. 42 (1999) 1273-1287.

[13] S.S. Kumar, P.M. Abilash, K. Ramamurthi, Thermal contact conductance for cylindrical and spherical contacts, Heat Mass Transf. 40 (2004) 679–688.

[14] G.R. Mcgee, M.H. Schankula, M.M. Yovanovich, Thermal resistance of cylinder-flat contacts: theoretical analysis and experimental verification of a line-contact model, Nuclear Engineering and Design. 86 (1985) 369-381.

[15] Dongmei, B., Chen, H., Ye, T., Influences of temperature and contact pressure on thermal contact resistance at interfaces at cryogenic temperatures, Cryogenics, 52 (2012), 403–409.

[16] C. Fieberg, R. Kneer, Determination of thermal contact resistance from transient temperature measurements, Int. J. Heat Mass Transf. 51 (2008) 1017–1023.

[17] J. Beck, K. Woodbury, Inverse problems and parameter estimation: integration of measurements and analysis, Meas. Sci. Technol. 9 (1998) 839–847.

[18] J. Beck, Combined parameter and function estimation in heat transfer with application to contact conductance, J. Heat Transfer. 110 (1988).

[19] H. Molavi, A. Hakkaki-Fard, R.K. Rahmani, A. Ayasoufi, M. Molavi, A novel methodology for combined parameter and function estimation problems, J. Heat Transfer. 132 (2010) 121301.

[20] O.M. Alifanov, Inverse Heat Transfer Problems, Springer-Verlag, Berlin Heidelberg 1994.

[21] C. Huang, M. Ozisik, B. Sawaf, Conjugate gradient method for determining unknown contact conductance during metal casting, Int. J. Heat Mass Transf. 35 (1992) 1779–1786.

[22] M.H. Shojaeefard, V.M. Khaneshan, M.M. Sharfabadi, The investigation of the valve spring stiffness influence on the thermal contact conductance between the exhaust valve and its seat, Heat Transf. Eng. 36 (2015) 58–67.

[23] E.M. Burghold, Y. Frekers, R. Kneer, Determination of time-dependent thermal contact conductance through IR-thermography, Int. J. Therm. Sci. 98 (2015) 148–155.

[24] E. M. Burghold, Y. Frekers, and R. Kneer, "Transient contact heat transfer measurements based on high-speed IR-thermography," Int. J. Therm. Sci., 115 (2017) 169–175.

[25] T. Chen, P. Tuan, Inverse problem of estimating interface conductance between periodically contacting surfaces using the weighting input estimation method, Numer. Heat Transf, Part B. (2002) 477–492.

[26] M.N. Ozisik, H.R.B. Orlande, Inverse Heat Transfer: Fundamentals and Applications, Taylor and Francis, New York, 2000.

[27] J.V. Beck, B. Blackwell, C.R. St. Clair, Inverse Heat Conduction. Ill- Posed Problems, Wiley-Verlag, New York, 1985.

[28] T.P.D. Rajan, K.N. Prabhu, R.M. Pillai, B.C. Pai, Solidification and casting/mould interfacial heat transfer characteristics of aluminum matrix composites, Composites Science and Technology. 67 (2007) 70–78.

[29] A. Plotkowski, M.J.M. Krane, The use of inverse heat conduction models for estimation of transient surface heat flux in electroslag remelting, J. Heat Transfer. 137 (2015).

[30] P. Fernandes, K.N. Prabhu, Comparative study of heat transfer and wetting behaviour of conventional and bioquenchants for industrial heat treatment, Int. J. Heat Mass Transf. 51 (2008) 526–538.

[31] B. Abdulhay, B. Bourouga, F. Alzetto, C. Challita, Development of an experimental procedure for thermal contact resistance estimation at the glass/metal contact interface, J. Therm. Sci. Eng. Appl. 6 (2014) 21006.

[32] Z. Zhu, L.W. Zhang, S.D. Gu, Experimental investigation of transient heat transfer between hastelloy C-276/narrow air gap/silicon steel, Exp. Therm. Fluid Sci. 45 (2013) 221–226.

[33] J. Beck, Nonlinear estimation applied to the nonlinear inverse heat conduction problem, Int. J. Heat Mass Transf. 13 (1970) 703–716.

[34] Z. Zhu, L. Zhang, C. Zhang, R. Li, S. Gu, Experimental investigation of transient contact heat transfer between 300M and 5CrNiMo, Int. J. Heat Mass Transf. 96 (2016) 451–457.

[35] M.K. Das, A. Tariq, P.K. Panigrahi and K. Muralidhar, Estimation of convective heat transfer coefficient from transient liquid crystal data using an inverse technique, Inverse Probl. Sci. Eng. 13 (2005) 133–155.

[36] R. James, K. Rowe, D. Gary, J. Lock, M. Owen, Transient heat transfer measurements using thermochromic liquid crystal: lateral-conduction error. Int. J Heat and Fluid Flow. 26 (2005) 256–263.

[37] H.S. Carslaw, J.C. Jaeger, Conduction of Heat in Solids, Oxford University Press, Amen House, London, 1959.

[38] J. G. Stoltz, "Numerical solution to an inverse problem of heat conduction for simple shapes," J. Heat Transfer. 82. (1960) 20-26.

[39] B. B. Mikic, W. M. Rohsenow, Thermal Contact Resistance. Massachusetts Institute of Technology, Rept. 4542-41, NASA Contract No. NGR-22-009-065, Sept. 1966.

[40] W.D.J. Callister, Materials Science and Engineering: An Introduction. sixth ed., John Wiley & Sons, 2003.

[41] J. Zheng, Y. Li, P. Chen, G. Yin, H. Luo, Measurements of interfacial thermal contact conductance between pressed alloys at low temperatures. Cryogenics, 80 2016 33–43.

[42] J. E. Shigley, Mechanical Engineering Design, third ed., McGraw Hill, Inc., New York, 1977.

[43] J.P. Holman, Experimental Methods for Engineers, seventh ed., Tata McGraw Hill, New Delhi, 2001, 51-60.

**Table 1** Data used in solving the direct problem

| | Body 1 | Body 2 |
|---|---|---|
| Specimen length, m | 0.03 | 0.03 |
| Thermal conductivity, W/m-K | 16 | 16 |
| Thermal diffusivity, $m^2/s$ | $4.09 \times 10^{-6}$ | $4.09 \times 10^{-6}$ |
| Initial Temperature, K | 300.15 | 373.15 |

**Table 2** Summary of properties and dimensions of specimens used in experiments

| Property | Hot Body | Cold Body |
|---|---|---|
| $E$, $N/m^2$ | $2.07\times10^{11}$ [40] | $2.07\times10^{11}$ [40] |
| $\nu$ | 0.30 [40] | 0.30 [40] |
| $k$, W/mK | 16.0 | 16.0 |
| $H$, MPa | 3095.76 | 3095.76 |
| $m$, μm | 4.73 | 5.79 |
| $\sigma$, radian | 0.462 | 0.457 |
| *Dimensi* | | |

| *ons* | | |
|---|---|---|
| Length, mm | 40.0 | 40.0 |
| Width, mm | 23.0 | 23.0 |
| Depth, mm | 22.5 | 22.5 |

**Table 3 Correlations to predict TCC**

| Model | Correlation |
|---|---|
| Mikic Plastic [2] | $h^* = 1.13\ (P^*)^{0.94}$ |
| Mikic and Rohsenow Plastic [39] | $h^* = 0.90\ (P^*)^{16/17}$ |
| Asif and Tariq [6] | $h^* = 0.72\ (P^*)^{0.95}$ |

**Table 4** Comparison of experimental transient TCC with steady state TCC

| **Initial Temperature,** °C (Cold Body/Hot Body) | $54 \pm 0.5 / 140 \pm 0.5$ | | | | | | | | | |
|---|---|---|---|---|---|---|---|---|---|---|
| **Contact configurations** | Flat-Flat | | | | Cylinder-Flat | | | Cylinder-Cylinder | | |
| **Loading,** kN | 0.63 | 3.35 | 5.00 | 6.25 | 0.60 | 5.20 | 6.30 | 0.65 | 5.00 | 6.30 |
| Stabilized Value of | **0.91** | **1.68** | **1.91** | **2.10** | **0.292** | **0.659** | **0.680** | **0.274** | **0.435** | **0.464** |

| $h(t)$, kW/m$^2$°C | | | | | | | | | | |
|---|---|---|---|---|---|---|---|---|---|---|
| $h_{\Delta T\_no\ extrp.}$, kW/m$^2$°C | 0.92 | 1.70 | 1.92 | 2.10 | 0.292 | 0.659 | 0.68 | 0.274 | 0.435 | 0.464 |
| $h_{\Delta T\_extrp.}$, kW/m$^2$°C | **1.31** | **3.47** | **4.11** | **5.27** | **0.305** | **0.714** | **0.739** | **0.286** | **0.463** | **0.497** |
| **Underprediction (%)** | **3.53** | **5.59** | **5.53** | **6.15** | **4.26** | **7.70** | **7.98** | **4.20** | **6.04** | **6.64** |

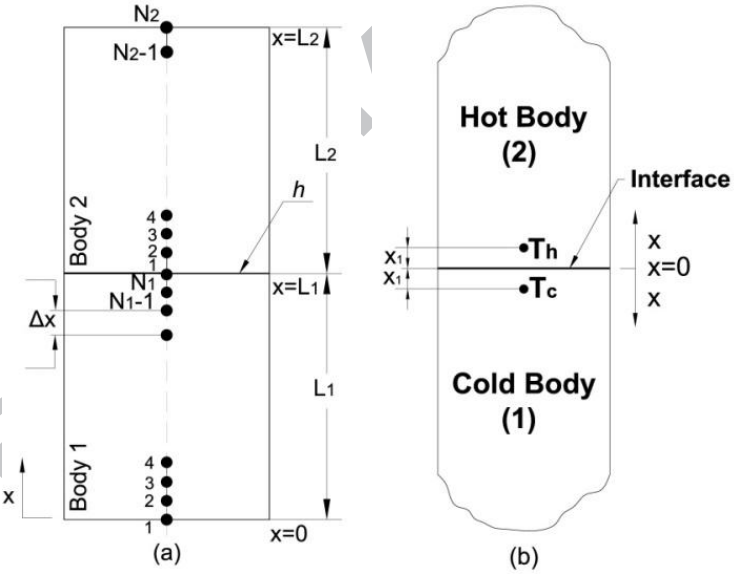

Fig. 1 Schematic of (a) 1-D geometry used in numerical simulation, and (b) two semi-infinite bodies in contact

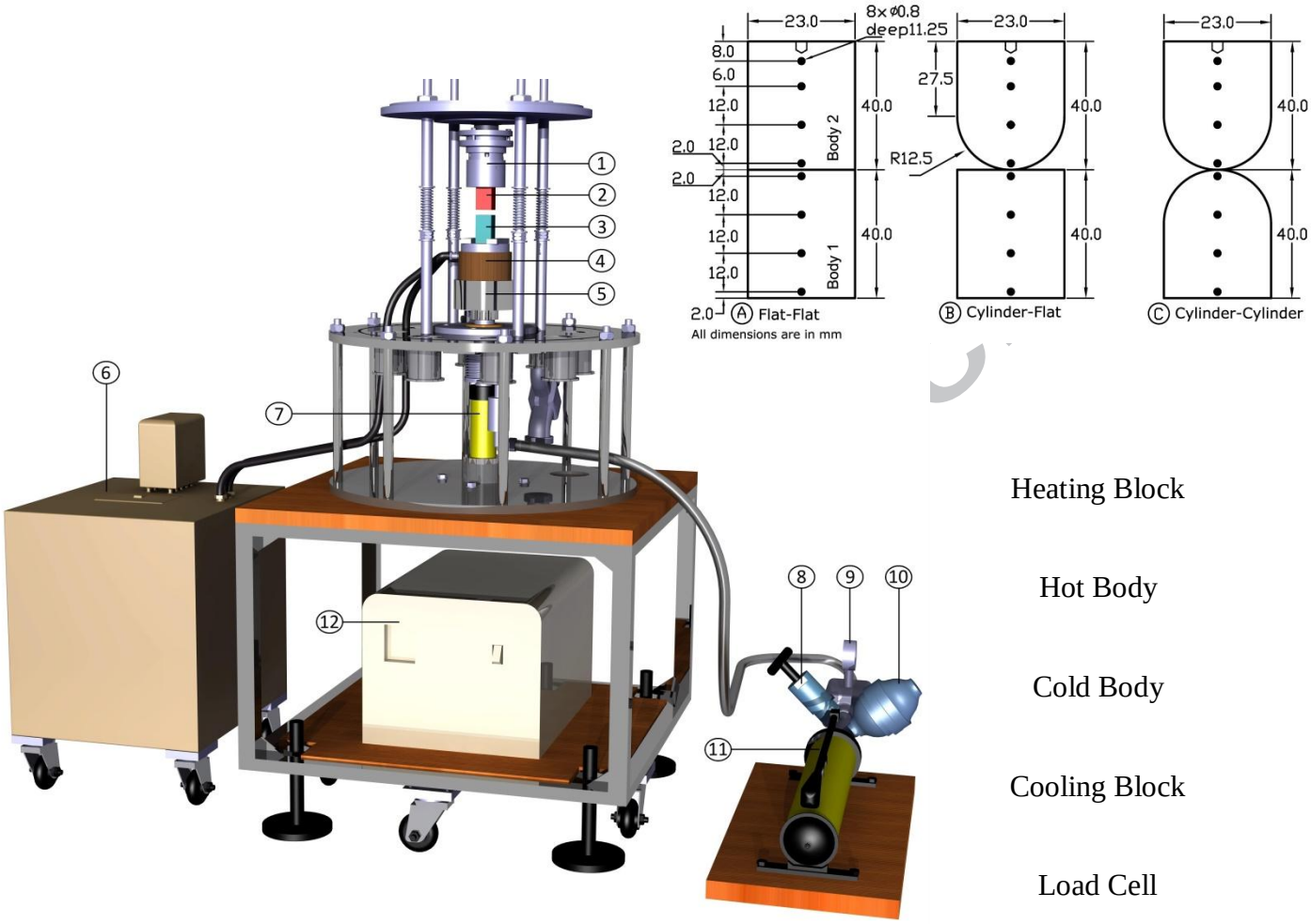


Heating Block

Hot Body

Cold Body

Cooling Block

Load Cell

PID Controlled Chiller

Hydraulic Jack

Check Valve

Pressure Gauge

Load

0 Accumulator



Hydraulic

1 Pump

Stabilized

2 Power Source

Fig. 2 Schematic diagram of experimental setup and specimens of different contact configurations

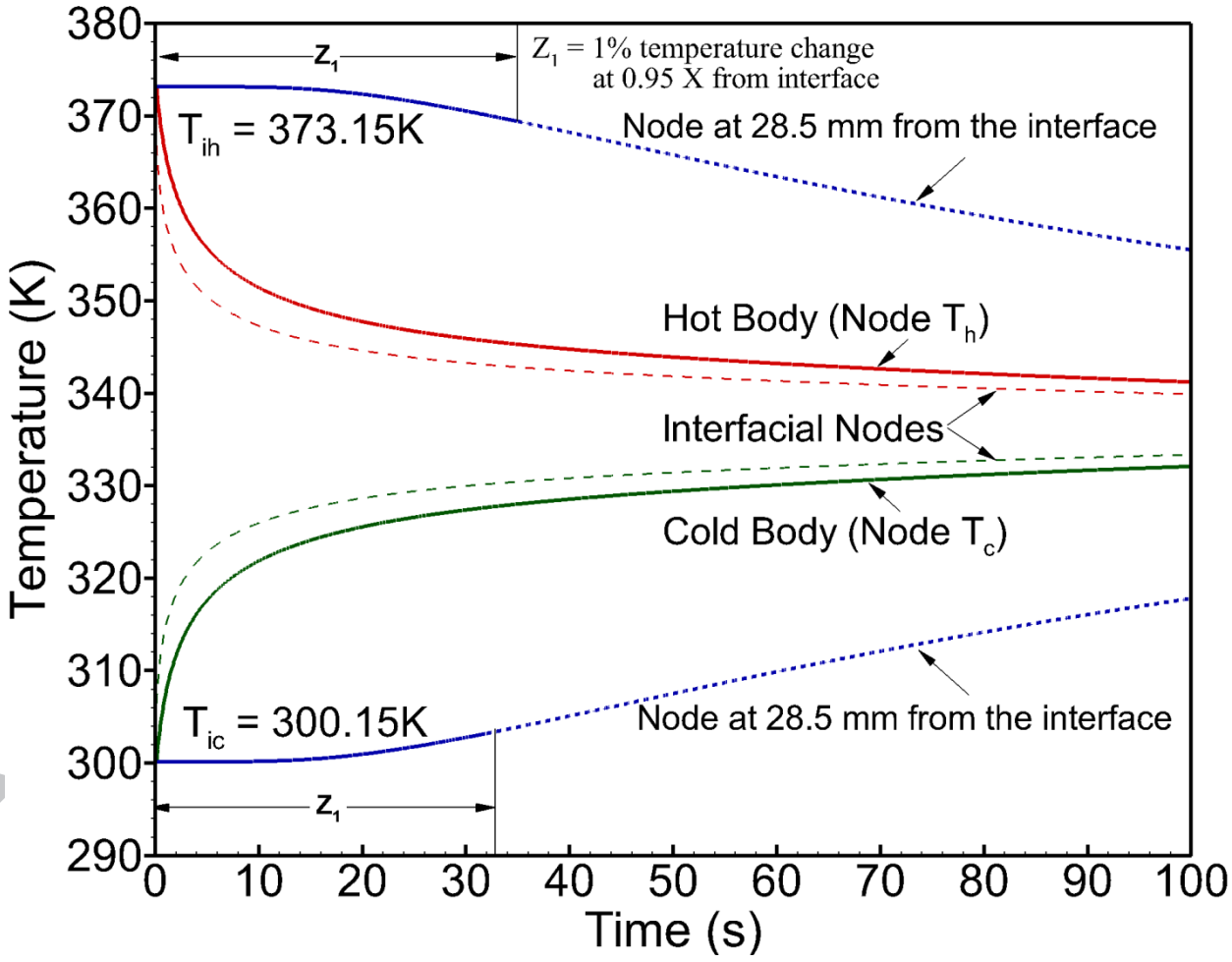

Fig. 3 Simulated temperature measurements at different axial locations from two contacting bodies

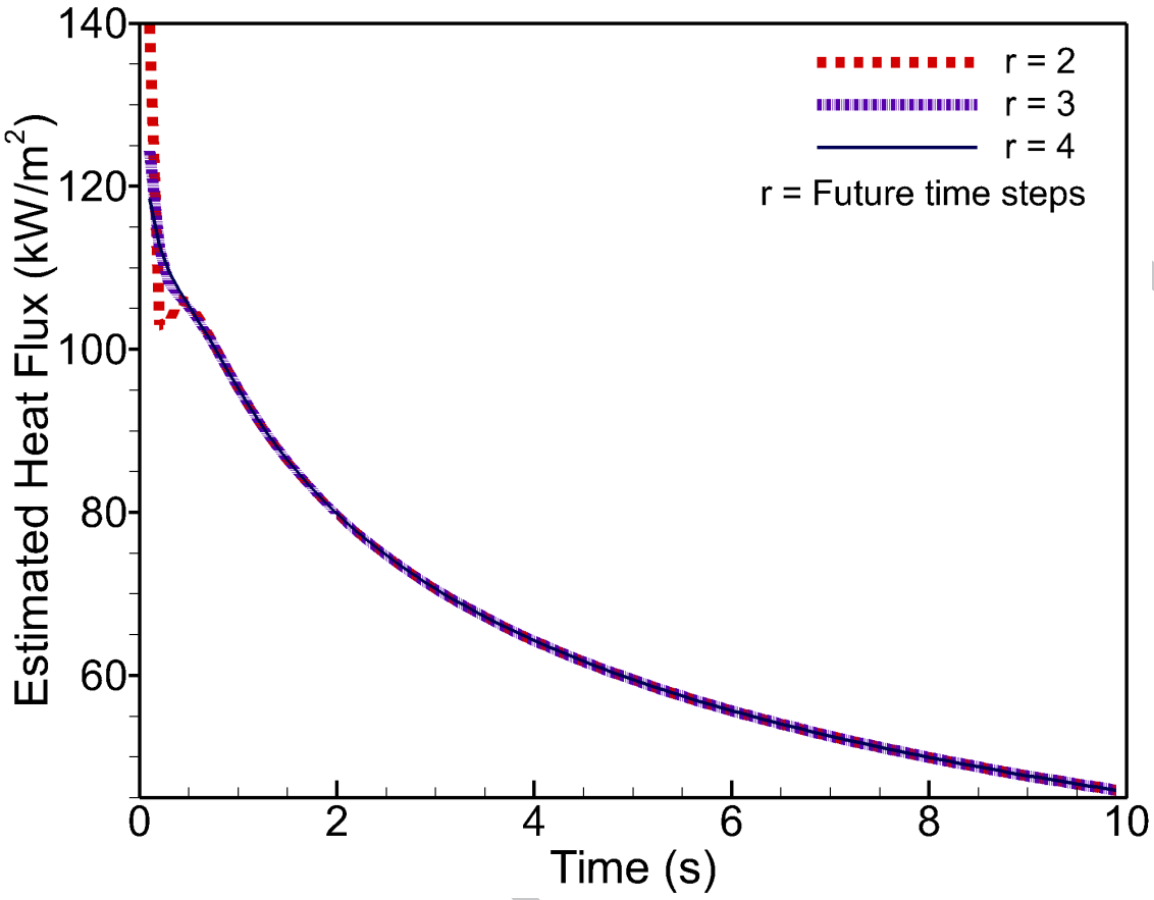


Fig. 4 Effect of future temperature steps in the estimation of interfacial heat flux

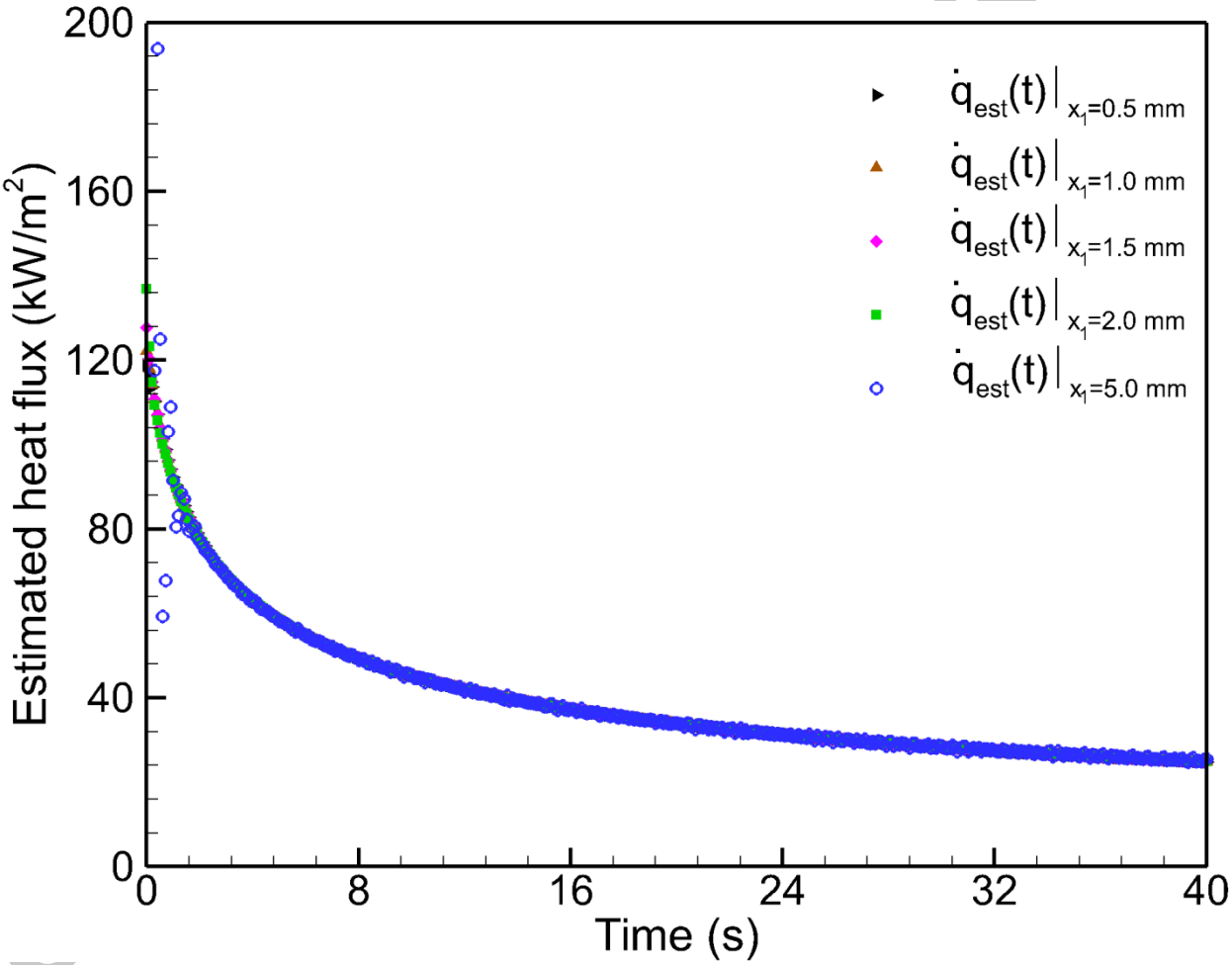


Fig. 5 Estimation of heat flux from simulated temperatures at different axial locations

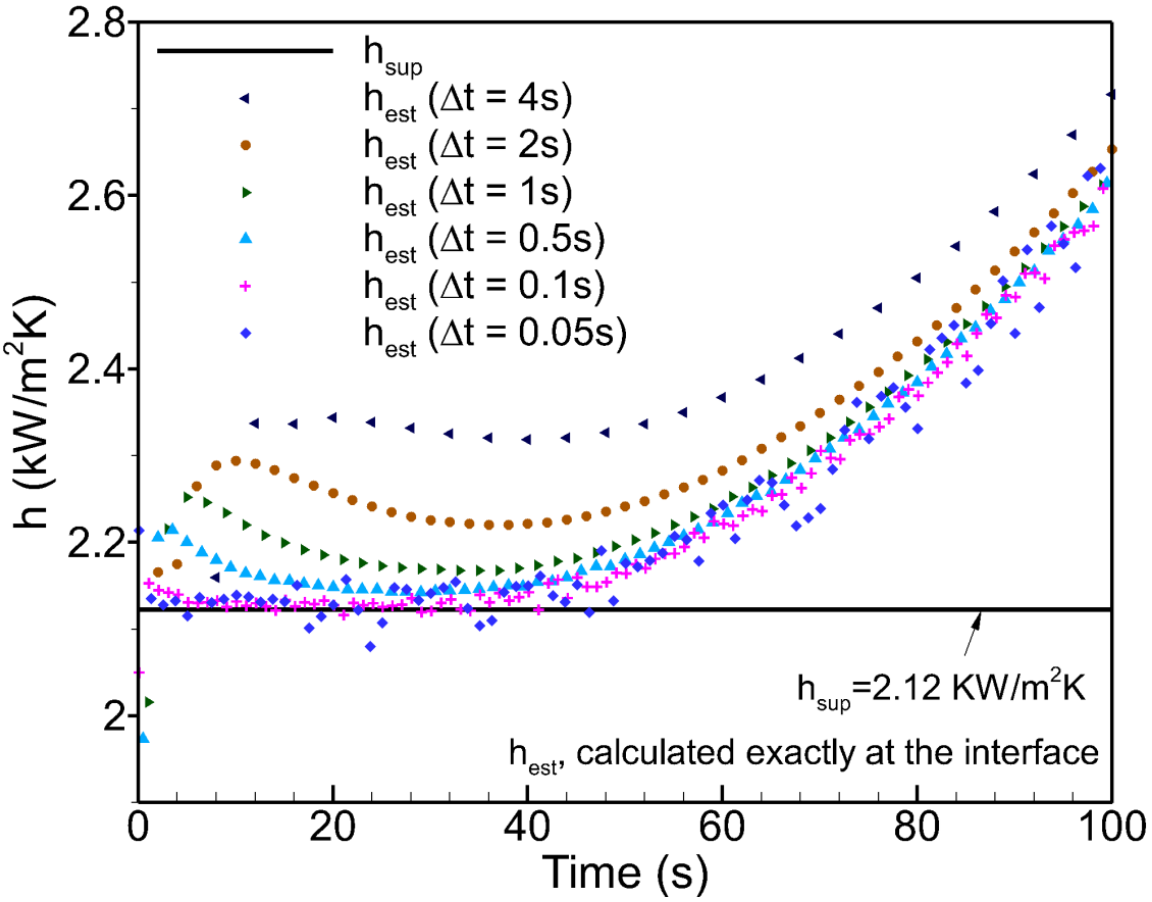

Fig. 6 Numerical estimation of TCC at varying time steps

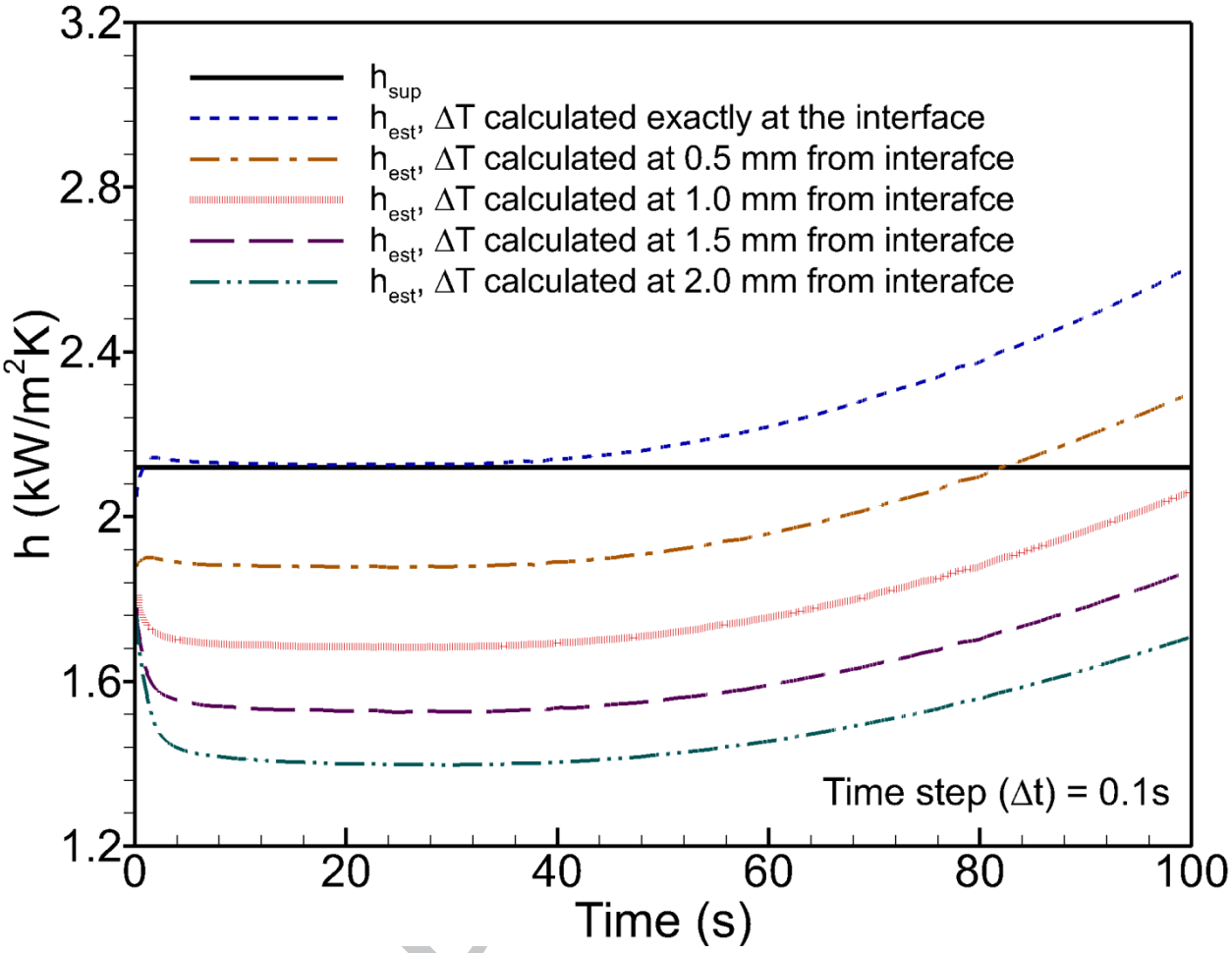


Fig. 7 Effect of interfacial temperature drop on the estimation of TCC from simulated temperatures

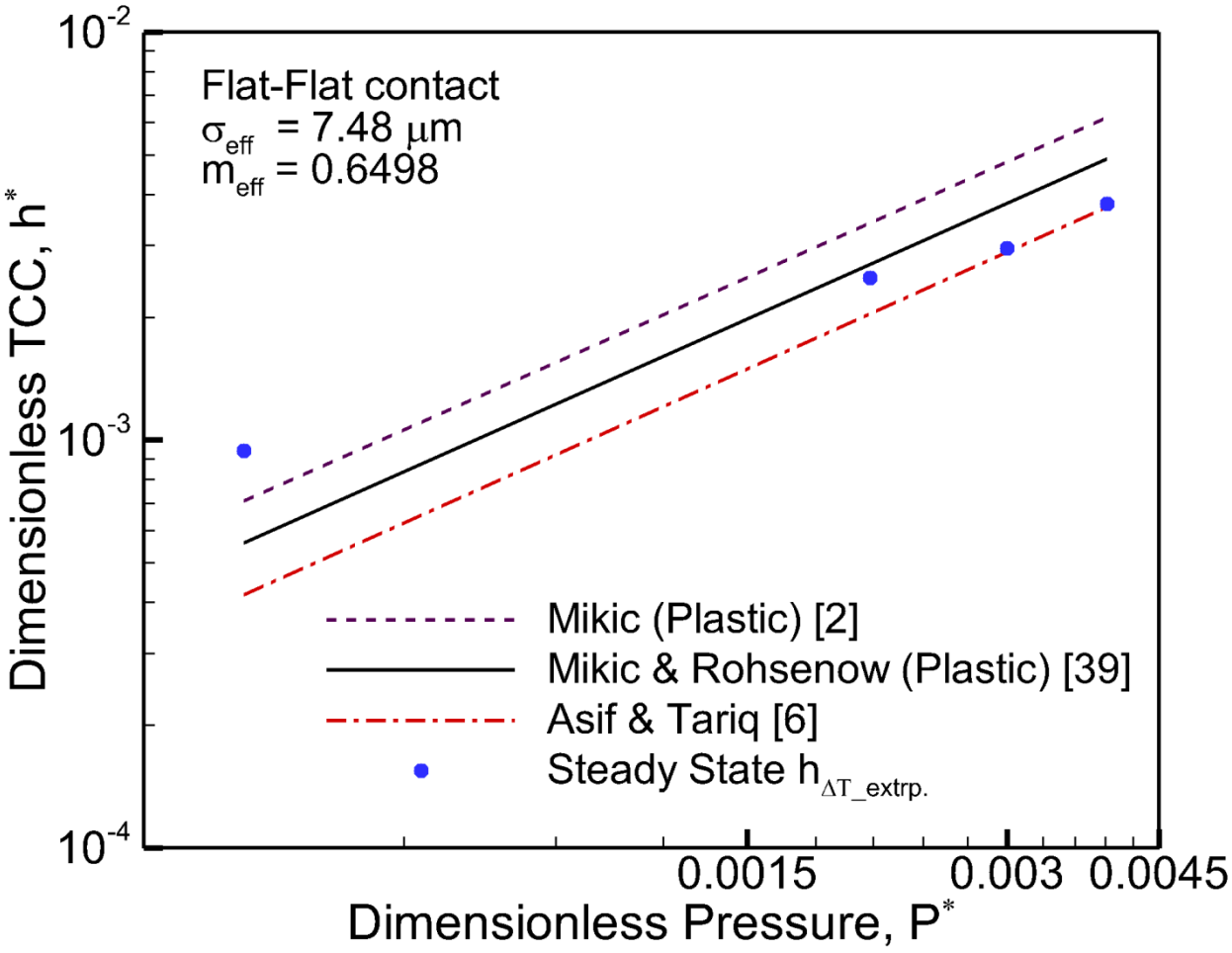


Fig. 8 Comparison of experimental steady state TCC with available correlations

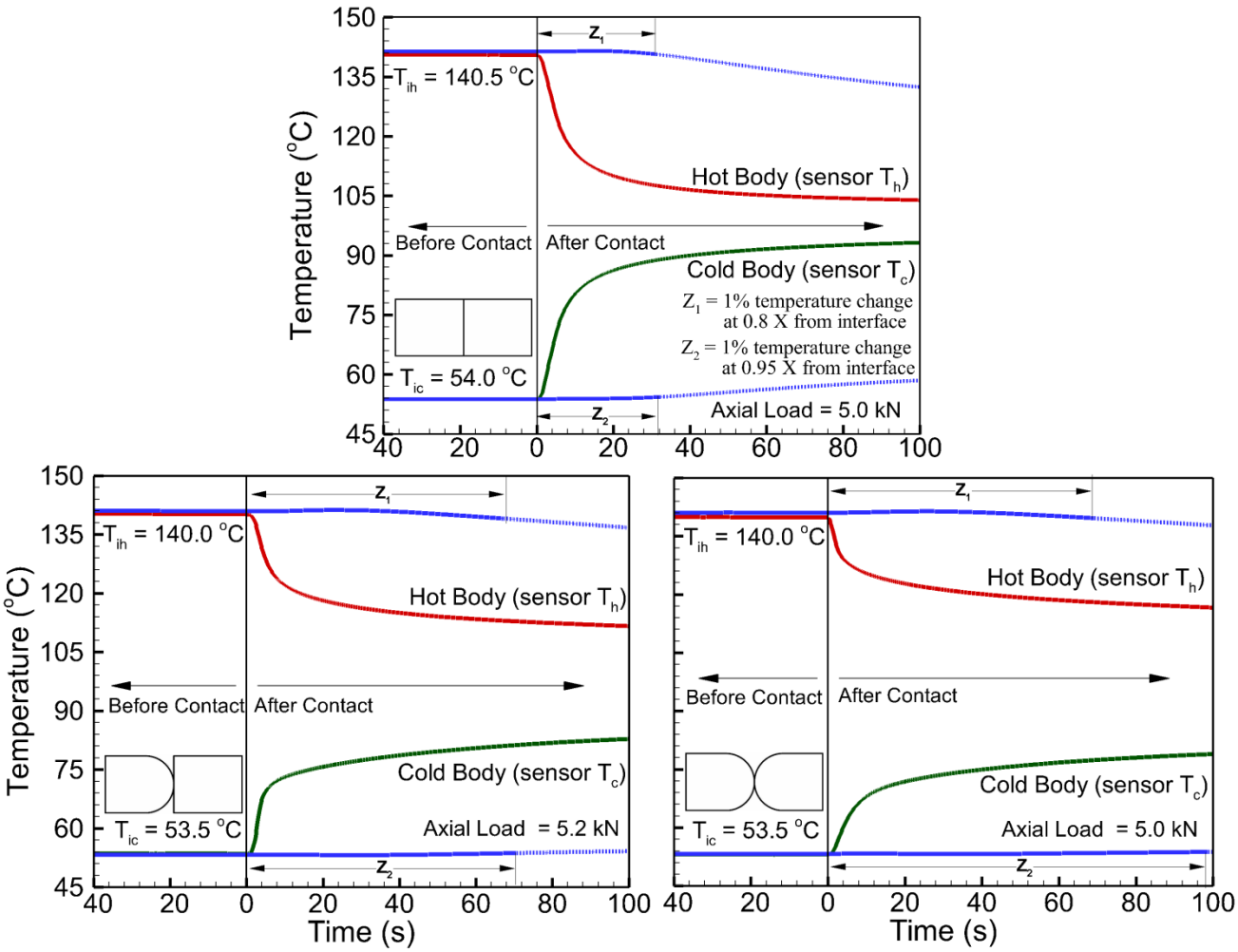


Fig. 9 A typical temperature transient of two points from interface in each specimen for different contact configurations under similar axial loading condition (□5.0±0.2 kN)

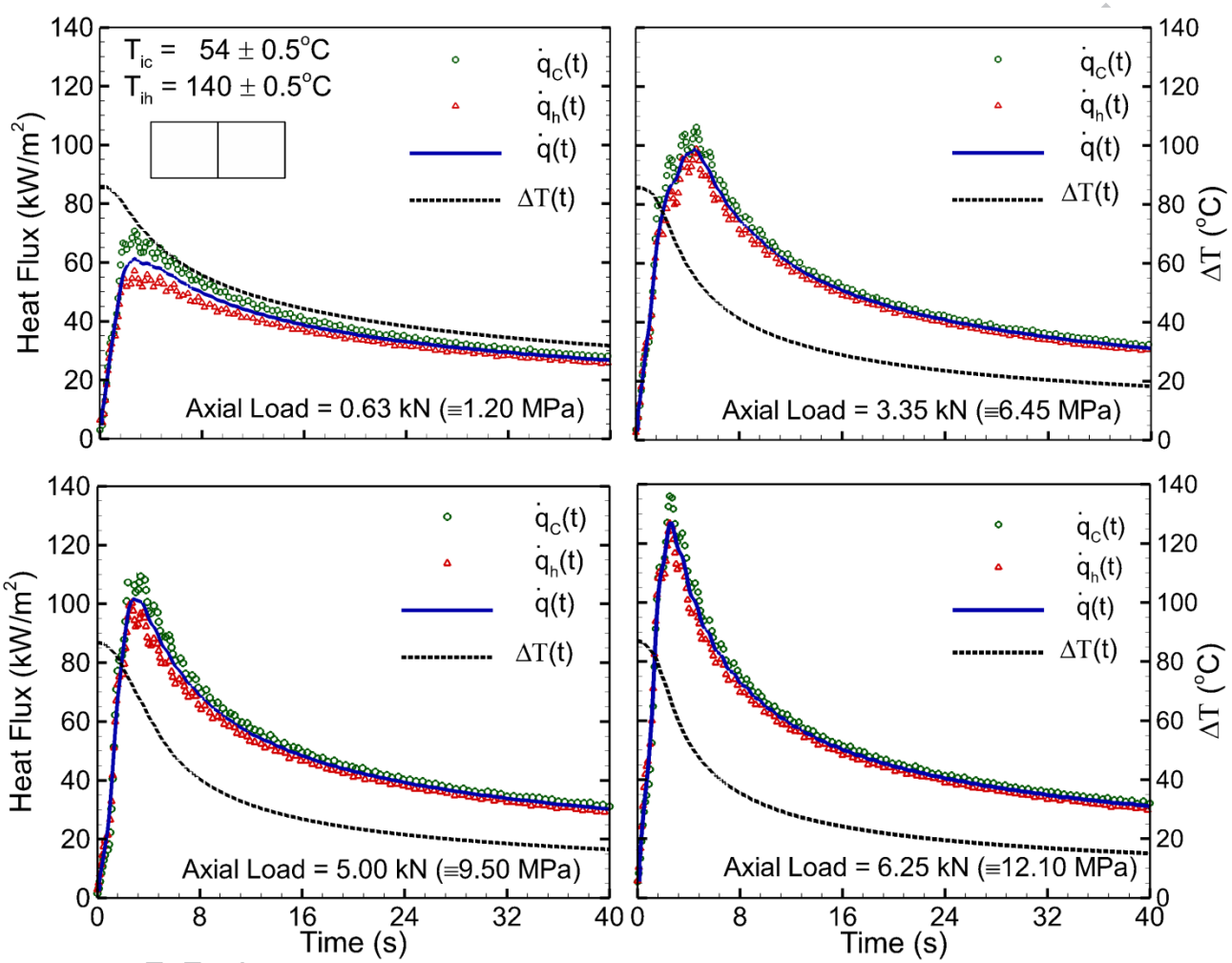


Fig. 10 Heat flux transient and interfacial temperature drop variation for flat-flat contact configuration under different loading conditions

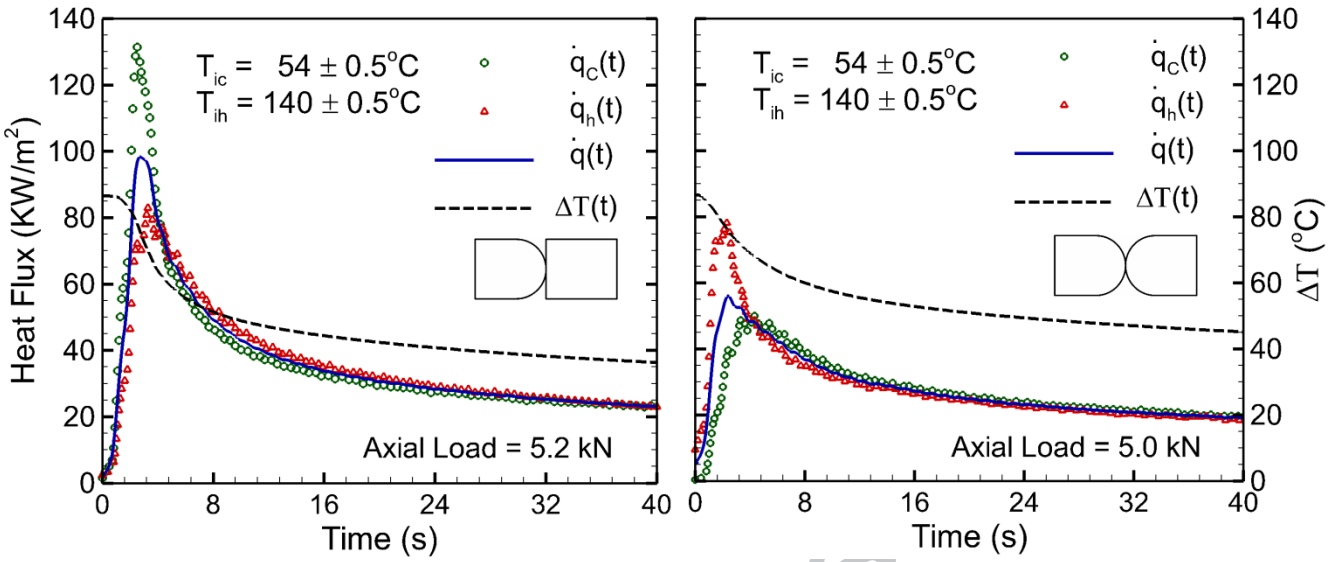


Fig. 11 Heat flux transient and interfacial temperature drop variation for curvilinear contacts under similar axial loading condition (□5.0±0.2 kN)

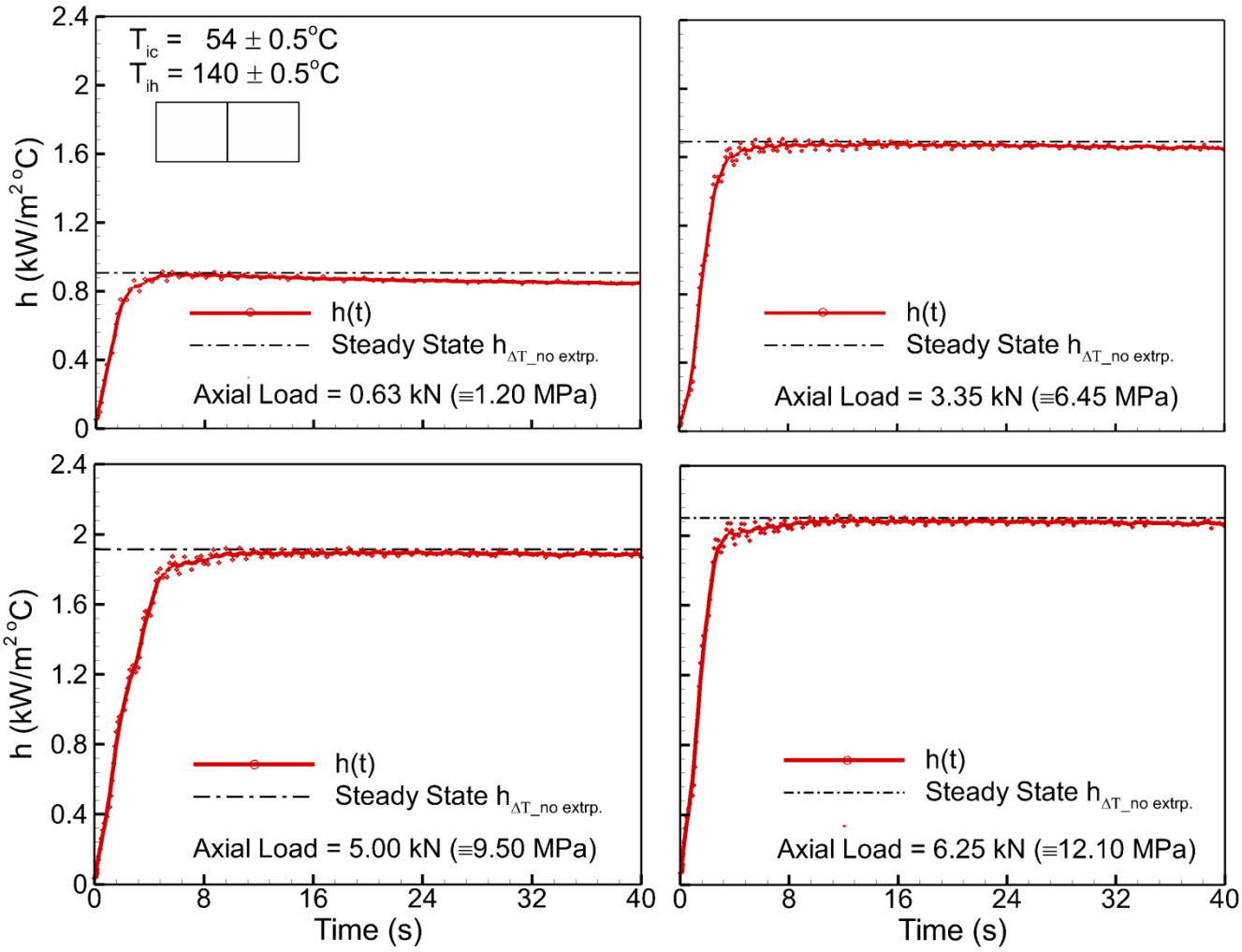


Fig. 12 Transient TCC for flat-flat contact configuration under different loading conditions

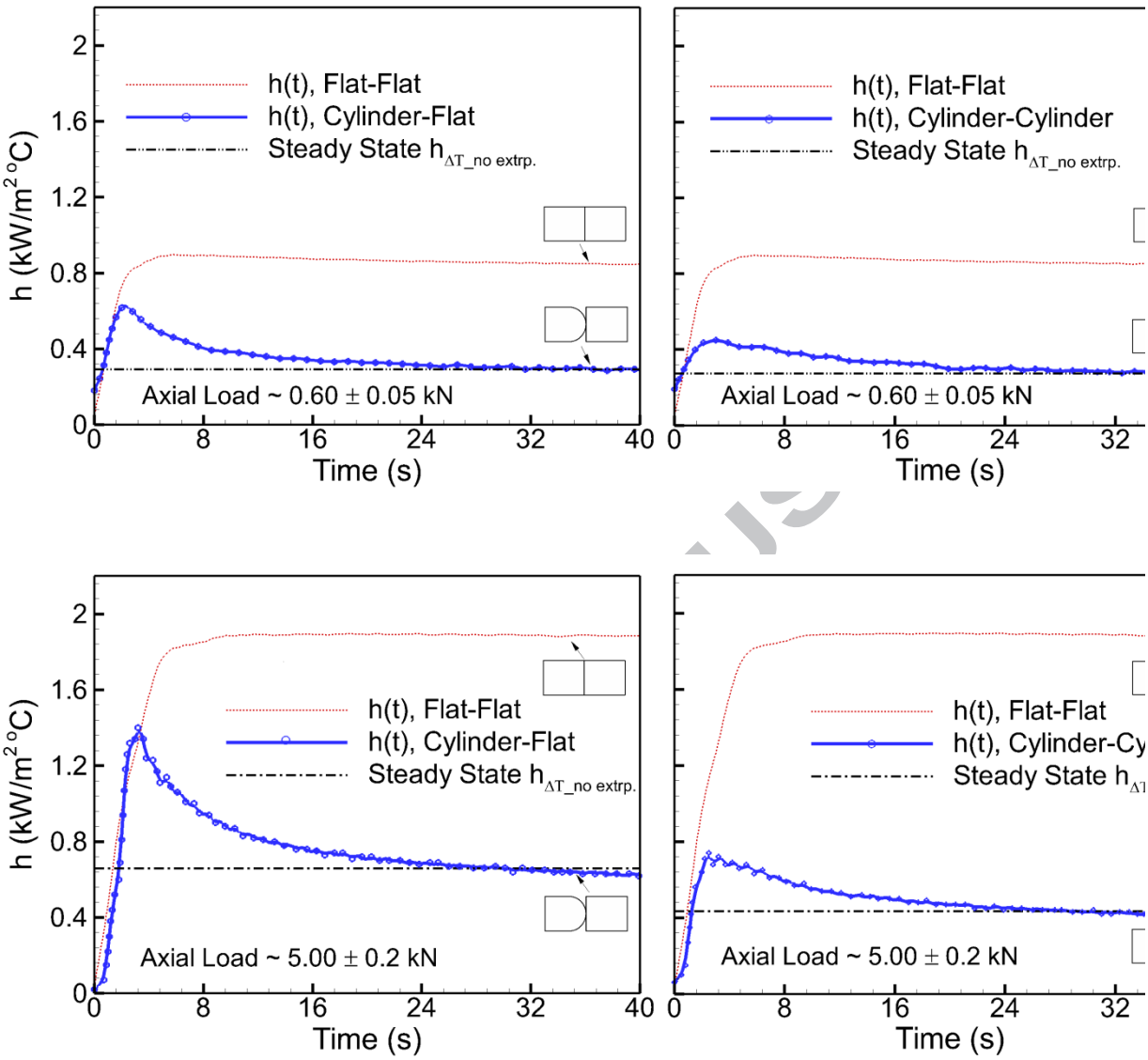

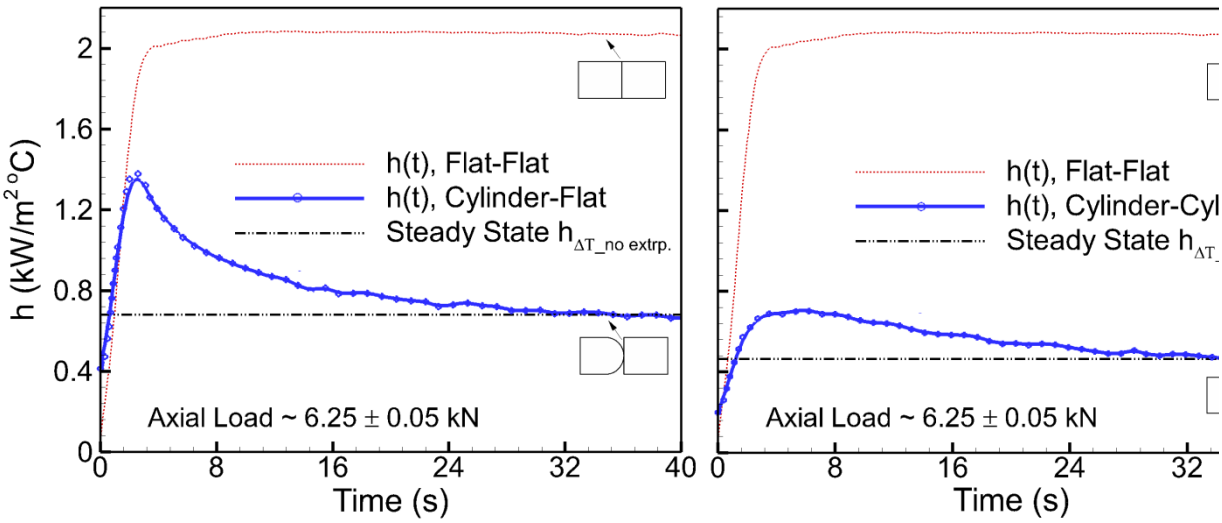


Fig. 13 Transient TCC for curvilinear contact configurations under different loading conditions

**Highlights**

- Determination of thermal contact conductance (TCC) by using an inverse transient approach with numerical and experimental measurements.
- Comparison between the transient and steady state TCC results for flat-flat, cylinder-flat and cylinder-cylinder contacts.
- A quasi-static equilibrium of the heat flow is observed within short duration based transient measurements, which is used to successfully extract the steady-state TCC estimate with greater reliability.
- Results of different-but exemplary- contact models offers the valuable insight of transient heat transfer at the interface.